

# Evaluation of Static Liquefaction Characteristics of Saturated Loose Sand Through the Mean Grain Size and Extreme Grain Sizes

Leila Hazout · Zein El-Abidine Zitouni · Mostefa Belkhatir · Tom Schanz

Received: 2 August 2016 / Accepted: 30 March 2017 / Published online: 7 April 2017  
© Springer International Publishing Switzerland 2017

**Abstract** Liquefaction of soils is a natural phenomenon associated with a dramatic loss of the soil shear strength in undrained conditions due to a development of excess pore water pressure. It usually causes extensive damages to buildings and infrastructures during earthquakes. Thus, it is important to evaluate extent of influential parameters on the liquefaction phenomenon of soils in order to clearly understand the different mechanisms leading to its triggering. The soil gradation is one of the most important parameters affecting the liquefaction phenomenon. In this context, a series of undrained compression triaxial tests were carried out on eighteen natural loose ( $D_r = 25\%$ ) sandy samples containing low plastic fines content of 2% ( $I_p = 5\%$ ) considering different extreme sizes ( $1.6 \text{ mm} \leq D_{\max} \leq 4 \text{ mm}$  and

$0.001 \text{ mm} \leq D_{\min} \leq 0.63 \text{ mm}$ ) and two mean grain size ranges ( $0.25 \text{ mm} \leq D_{50} \leq 1.0 \text{ mm}$ ) and ( $1.0 \text{ mm} \leq D_{50} \leq 2.5 \text{ mm}$ ). The initial confining pressure for all tests was kept constant ( $P'_c = 100 \text{ kPa}$ ). The obtained test results indicate that the mean grain size ( $D_{50}$ ) and extreme grain sizes ( $D_{\max}$  and  $D_{\min}$ ) have a significant influence on the undrained shear strength (known as liquefaction resistance) and appear as pertinent factors for the prediction of the undrained shear strength for the soil gradation under study. The undrained shear strength and the excess pore water pressure can be correlated to the extreme grain sizes ( $D_{\max}$  and  $D_{\min}$ ) and the mean grain size ( $D_{50}$ ) of tested wet deposited samples.

**Keywords** Mean grain size · Extreme grain sizes · Static liquefaction · Saturated sandy soil · Wet deposition method

L. Hazout · Z. El-Abidine Zitouni  
Saâd Dahlab University of Blida, Faculty of Technology,  
Civil Engineering Department, B.P 270 RP, Route de  
Soumaa, 09000 Blida, Algeria

M. Belkhatir (✉)  
Laboratory of Materials Sciences and Environment,  
Hassiba Benbouali University of Chlef, BP 151, Route de  
Sendjes, 02000 Chlef, Algeria  
e-mail: abelkhatir@yahoo.com

M. Belkhatir · T. Schanz  
Laboratory of Foundation Engineering, Soil and Rock  
Mechanics, Department of Civil and Environmental  
Engineering Ruhr-Universität Bochum, Bochum,  
Germany

## Abbreviations

$A_i, B_i$ and $C_i$	Soil samples of group 01
$D_i, E_i$ and $F_i$	Soil samples of group 02
$a, c$	Coefficients of equation
$B$	Skempton's pore pressure parameter
$C_u$	Coefficient of uniformity
$C_c$	Coefficient of curvature
$D$	Diameter of the sample
$D_{\max}$ and $D_{\min}$	Extreme grain sizes
$D_{10}$	Effective grain size
$D_{50}$	Mean grain size

$D_r$	Initial relative density
$e_i$	Initial void ratio of sample reconstitution
$e_c$	Post-consolidation void ratio of sample reconstitution
$e_{\max}$ and $e_{\min}$	Extreme void ratios of the sand matrix
$G_s$	Specific gravity of solids
$H$	Height of the sample
$H/D$	Height to diameter ratio of the sample
$P'_c$	Initial confining pressure
$q_{\max}$	Maximum shear strength
$R^2$	Coefficient of determination
USCS	Unified Soil Classification System
$w$	Water content
$\Delta u_{\max}$	Maximum positive excess pore water pressure
$\Delta e = e_{\max} - e_{\min}$	Difference between extreme void ratios
$\Delta e_c = e_i - e_c$	Difference between initial void ratio and post-consolidation void ratio

## 1 Introduction

The Chlef region located in northern Algeria (Fig. 1) was affected by a strong earthquake on October 10th, 1980. It was the most destructive and damaging earthquake that affected the City of Chlef (formerly known as El-Asnam) and surrounding areas. This quake with Richter Magnitude,  $M_L = 7.2$ , corresponding to a Surface Wave Magnitude,  $M_s = 7.3$  generated significant damages of varying extents to a large number of small to moderate size civil and hydraulic structures in the vicinity of the earthquake epicenter (Belkhatir et al. 2012). Belkhatir et al. (2012) reported that important ground deformations in terms of lateral spreading, flow failures, ground fissures and subsidence, sand boils, and slope failures were observed. The earthquake epicenter of the main shock was located 12 km in the east region of Chlef City (210 km west of Algiers) at latitude 36.143N and longitude 1.413E with a focal depth of about 10 km. The earthquake duration lasted 35 s at the end of which much of the city and surrounding areas up to a distance of 60 km were in ruins. This event,



**Fig. 1** Location of El Asnam (Area of study)

commonly referred to as the 1980 El Asnam Earthquake, was one of the most destructive earthquakes recorded in northern Africa and more largely in the Western Mediterranean Basin that have affected the northern region of Algeria. The earthquake devastated the city of El Asnam, population estimated at 125,000, and the nearby towns and villages. The large loss of life (reportedly 5000–20,000 casualties) and property was attributed to the collapse of buildings (Fig. 2). In several places of the affected area, especially along Chlef river banks great masses of sandy soils were ejected on to the ground surface level. Significant damages to civil and hydraulic structures (earthdams, embankments, bridges, slopes and buildings) were caused by this earthquake (Belkhatir et al. 2012).

## 2 Literature Review

The shear strength, deformation and settlement characteristics of sandy soil deposits are significantly affected by the generated excess pore water pressure due to earthquake loading conditions. Therefore, the safety of the civil engineering and hydraulics structures constructed from these deposits or founded on them is adversely influenced. Soil liquefaction is one of the most important earthquake-induced hazards. During earthquake shaking or dynamic shearing, the



**Fig. 2** Recorded building damages during 1980 El Asnam earthquake. **a** Medical clinic. **b** Algerian gallery store. **c** Primary school canopy

undrained shear strength of saturated sandy soils decreases due to a rapid buildup of excess pore water pressure within a short time. When the excess pore pressure reaches the initial consolidation pressure level, the effective stress becomes zero, inducing a partial or a complete shear strength loss, called initial liquefaction. At the state of initial liquefaction, the soil mass behaves as a liquid, causing tremendous damages to soil foundations and earth structures. Sand boils, settlement or tilting of structures, failures of earth dams and slopes, lateral spreading of bridge foundations, landsliding and soil subsidence are some examples of liquefaction damages (Belkhatir et al. 2014). Soil liquefaction usually occurs in saturated sandy soil deposits subjected to monotonic or dynamic loading conditions and it represents one of the most important and challenging research topics in the field of geotechnical earthquake engineering. Laboratory studies on soil liquefaction were initiated following the liquefaction induced failures observed after two subsequent earthquakes occurred in Niigata (Japan) and Alaska (USA) in 1964. Several researches (Zlatovic and Ishihara 1995; Lade and Yamamuro 1997; Thevanayagam et al. 1997; Thevanayagam 1998; Yamamuro and Lade 1998; Amini and Qi 2000; Naeini 2001; Naeini and Baziar 2004; Sharafi and Baziar 2010; Belkhatir et al. 2010; Della et al. 2011; Djafar Henni et al. 2011; Missoum et al. 2011; Bayat and Bayat 2012; Igwe et al. 2012; Janalizadeh et al. 2013; Abouzar Sadrekarimi 2013; Jafarian et al. 2013; Yanrong 2013; Benghalia et al. 2014; Sze and Yang 2014; Liu et al. 2014) have been reported on different factors controlling the soil liquefaction phenomenon. The effect of parameters such as the confining pressure, relative density, sample preparation, sample size and degree of saturation are well known. However, the influence of other variables including the soil

structure, grading characteristics, size, shape, distribution and packing of the particles is incomplete and requires further investigation. Lee and Fitton (1968) found that grain size distribution has a remarkable effect on the cyclic shear strength of the soil. Seed and Peacock (1971) concluded that the stress ratio causing liquefaction decreased as the effective diameter reduced from 1.0 to 0.1 mm. Some other researchers (Finn et al. 1970; Ishihara et al. 1975; Miura et al. 1994) showed that as particle size increased, the cyclic resistance increased. Seed and Idriss (1971) reported that for fine sand with  $D_{50}$  value around 0.08 mm is more susceptible to liquefaction. Castro and Poulos (1977) showed that uniform clean and loose sand was more vulnerable to liquefaction. Also, Chang et al. (1982) reported that cyclic liquefaction resistance of clean sand was strongly influenced by the mean grain size ( $D_{50}$ ), and the uniformity coefficient ( $C_u$ ), provided that  $D_{50} \leq 0.23$  mm. However, the individual influences of  $D_{50}$  and  $C_u$  were not isolated. Vaid et al. (1991) investigated the effect of the coefficient of uniformity ( $C_u$ ) on the undrained cyclic shear strength of three sandy samples reconstituted with the same mean grain size ( $D_{50}$ ) and they concluded that their cyclic liquefaction resistance increased with the increase of the coefficient of uniformity ( $C_u$ ) at low relative densities and the inverse tendency was observed at high relative densities. Miura et al. (1997) reported that maximum and minimum void ratio  $e_{max}$  and  $e_{min}$  were significantly affected by the grain size distribution and grain shape. Both  $e_{max}$  and  $e_{min}$  decrease with an increase in mean grain size ( $D_{50}$ ) or uniformity coefficient ( $C_u$ ). They found that the value of the extreme void ratios ( $e_{max}$  and  $e_{min}$ ) increases with the increase of the angularity. Moreover, they claimed that the glass beads gave the lowest value of  $e_{max}$  and  $e_{min}$ , because of their sphericity, size

uniformity and surface smoothness. Cubrinovski and Ishihara (2002) found that the maximum and minimum void ratios as well as the void ratio range were significantly affected by the particle shape in a way that these void ratios increased with increasing angularity or decreasing roundness of the particles. The void ratio range included the combined effects of mean grain size, grain size distribution, fines content and particle shape. In general ( $e_{\max}$  and  $e_{\min}$ ) can provide valuable and unique information about the material properties of sandy soils and they can be particularly effective in evaluating the potential of compressibility and contractiveness of cohesionless soils. Kokusho et al. (2004) showed that the post-liquefaction undrained strength was dependent on particle gradation and relative density for larger strain 20–25%, as soils with larger coefficient of uniformity ( $C_u$ ) and larger relative density ( $D_r$ ) lead to show larger undrained strength. They reported also that the undrained monotonic shear strength defined at larger strains after undrained cyclic loading was at least eight times larger for well-graded soils than poorly graded sand despite the same relative density. This indicates that devastating failures with large post liquefaction soil strain are less likely to develop in well-graded granular soils compared to poorly graded sands with the same relative density, although they are almost equally liquefiable. Kanagalingam and Thevanayagam (2005) examined the meaning of the parameter ‘b’ which “represents the participation of fines content in the internal contact force chain in the sand–silt mixtures” and they found this factor depends to coarse and silt grains characteristics ( $R_d = D_{50\text{sand}}/d_{50\text{silt}}$ ,  $C_{uc} = d_{60\text{sand}}/d_{10\text{sand}}$  and  $C_{uf} = d_{60\text{silt}}/d_{10\text{silt}}$ ), where these parameters have different influences on ‘b’. Monkul and Yamamuro (2011) investigated the fines content influence on liquefaction potential of a single base sand mixed with three different essentially nonplastic silts through strain-controlled monotonic undrained triaxial compression tests. Fines content was varied, to solely focus on how different silts and their contents influence the undrained response of the sand under comparable conditions. It was found that if the mean grain diameter ratio ( $D_{50\text{-sand}}/d_{50\text{-silt}}$ ) of the sand grains to silt grains was sufficiently small, the liquefaction potential of the sand increased steadily with increasing fines content for the studied range (0%–20%). As  $D_{50\text{-sand}}/d_{50\text{-silt}}$  increased, the liquefaction potential of the silty sand might actually be less

than the liquefaction potential of the clean sand and these results were valid for the selected confining stress (30 kPa) and deposition method. Yilmaz et al. (2008) and Choobbasti et al. (2013) found that the cyclic resistance of the soil could be expressed in terms of the grain sizes (i.e.,  $D_{10}$ ,  $D_{30}$ , or  $D_{60}$ ) rather than the coefficient of uniformity ( $C_u$ ) or the coefficient of curvature ( $C_c$ ) of the soil. In addition, Belkhatir et al. (2011) indicated that the undrained shear strength at the peak and the undrained residual shear strength could be correlated to  $C_u$  and  $D_{50}$ . In other words, the undrained shear strength at the peak and the undrained residual shear strength decreased linearly as the uniformity coefficient increased and the mean grain size decreased. They concluded that the liquefaction resistance could be expressed in terms of grading characteristics ( $D_{10}$ ,  $D_{50}$  and  $C_u$ ) rather than the coefficient of curvature ( $C_c$ ). Belkhatir et al. (2014) showed that the granulometric characteristics have an important influence on the generation of the excess pore water pressure of sand–silt mixture samples. Indeed, they found that the excess pore water pressure ( $\Delta u_{\max}$ ) could be correlated to the grading characteristics [ $D_{10}$ ,  $D_{50}$ ,  $C_u$ , effective size ratio (ESR), mean grain size ratio (MGSR) and Coefficient of uniformity ratio (CUR)]. Cherif Taiba et al. (2016) indicated that the gradation and particle shape affected in significant manner the undrained shear strength (known as the static liquefaction resistance) of Chlef (Algeria) and Fontainebleau (France) silty sand soils. Moreover, their test results confirmed the existence of simple correlations between liquefaction resistance and different grading characteristics ( $D_{10}$ ,  $D_{30}$ ,  $D_{50}$ ,  $D_{60}$ , and  $C_u$ ) of the soils under consideration and they introduced new soil granulometric ratios ( $D_{10R} = D_{10\text{sand}}/D_{10\text{mixture}}$ ,  $D_{50R} = D_{50\text{sand}}/D_{50\text{mixture}}$ , and  $C_{UR} = C_{usand}/C_{umixture}$ ) to discuss the sand–silt mixture liquefaction resistance susceptibility response. They concluded that the used grading characteristics ratios ( $D_{10R}$ ,  $D_{50R}$  and  $C_{UR}$ ) appeared as pertinent factors for the prediction of the undrained shear strength of the sand–silt mixtures. The study conducted by (Chang et al. 2016) showed that the variation of maximum void ratio with respect to fines content of a sand–silt mixture was caused by the same mechanisms that influence the variation of minimum void ratio. Consequently, a mathematical model proposed by the authors for predicting minimum void ratios of sand–silt mixtures was extended to be capable of predicting



the maximum void ratios of sand–silt mixtures due to the influence of fines content. The applicability of that model was verified by data from 24 sand–silt mixtures with various fines contents. Furthermore, the relationship between the maximum and the minimum void ratios of a sand–silt mixture could be derived. The derived relationship was found to be linear and was a function of fines content. The validity of the derived linear relationship between the maximum and the minimum void ratios of a sand–silt mixture was also verified by the measured results from experiments. Monkul et al. (2016) reported that base sand gradation had significant influence on the static liquefaction potential of clean and silty sands. They observed that clean sands became more liquefiable as their mean grain size got smaller and/or they became more uniform. However, they found that the order of liquefaction resistance of the same base sands were reversed when they were mixed with silt (i.e. resulting silty sands became more liquefiable as the mean grain size of base sand got larger and/or base sand became relatively well graded).

The main objective of this experimental investigation is to study the impact of gradation in terms of extreme grain sizes ( $D_{\max}$  and  $D_{\min}$ ) and different mean grain sizes ( $D_{50}$ ) on the undrained shear strength (known as static liquefaction resistance) response of

eighteen natural sandy samples containing 2% low plastic fines content and mixed with 5% of water ( $w = 5\%$ ). Therefore, the first group of samples were prepared with different extreme grain sizes ( $1.6 \text{ mm} \leq D_{\max} \leq 4.0 \text{ mm}$  and  $D_{\min} = 0.0016 \text{ mm}$ ) and mean grain sizes ( $0.25 \text{ mm} \leq D_{50} \leq 1.0$ ) and the second group of samples with ( $D_{\max} = 4.0 \text{ mm}$  and  $0.0016 \text{ mm} \leq D_{\min} \leq 0.63 \text{ mm}$ ) and mean grain sizes ( $1.0 \text{ mm} \leq D_{50} \leq 2.5 \text{ mm}$ ) reconstituted with a fabric technique termed “wet deposition” method at an initial relative density ( $D_r = 25\%$ ) and subjected to a constant confining pressure  $P'_c = 100 \text{ kPa}$ .

### 3 Experimental Program

#### 3.1 Index Properties of Tested Materials

The soil material used in this laboratory investigation was extracted from liquefied soil deposit areas along the banks of Chlef River where liquefaction cases were recorded during the 1980 El Asnam earthquake (Fig. 1). Chlef sand has been used in the preliminary tests as well as in triaxial tests presented in this laboratory research work. The tested materials were classified according to the (USCS: Unified Soil Classification System) as poorly graded sand. Figure 3

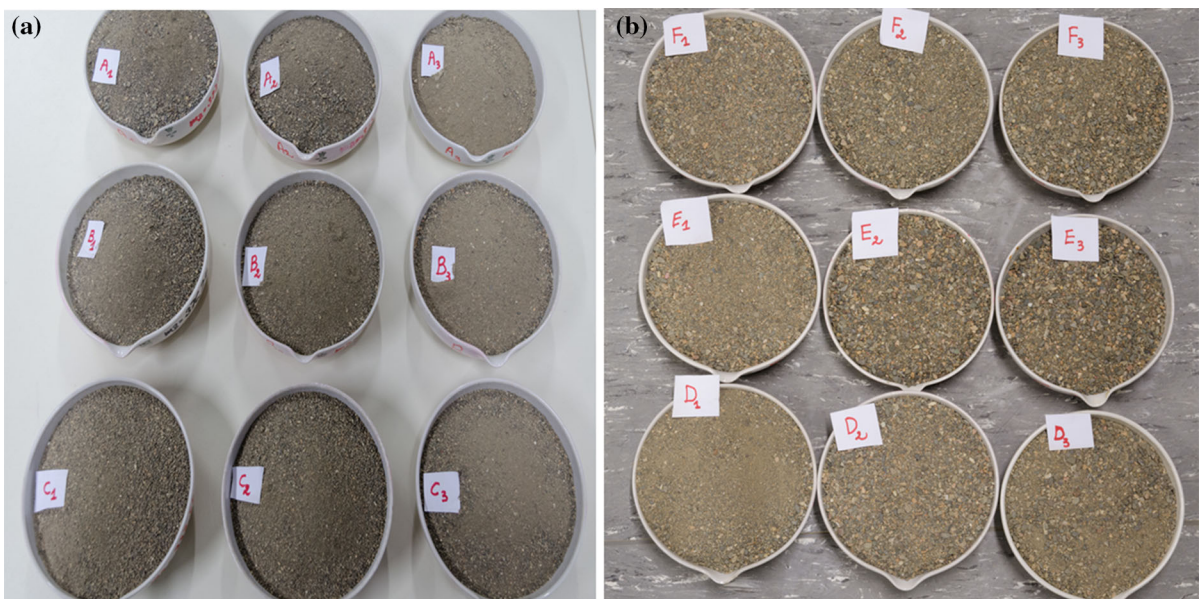


**Fig. 3** View of tested materials. **a** Group 1 ( $1.6 \text{ mm} \leq D_{\max} \leq 4.0 \text{ mm}$ ,  $D_{\min} = 0.0016 \text{ mm}$ ). **b** Group 2 ( $D_{\max} = 4.0 \text{ mm}$ ,  $0.0016 \text{ mm} \leq D_{\min} \leq 0.63 \text{ mm}$ )

**Table 1** Index properties of tested materials

	Sample	$G_s$	$D_{max}$ (mm)	$D_{min}$ (mm)	$D_{10}$ (mm)	$D_{50}$ (mm)	$C_u$	$C_c$	$e_{max}$	$e_{min}$
Group 1	A <sub>1</sub>	2.657	4	0.0016	0.302	1.00	4.28	1.2	0.746	0.537
	A <sub>2</sub>	2.655			0.19	0.63	5.32	0.9	0.71	0.477
	A <sub>3</sub>	2.650			0.12	0.25	4.34	0.6	0.709	0.467
	B <sub>1</sub>	2.664	2.5		0.28	1.00	4.1	1.25	0.798	0.532
	B <sub>2</sub>	2.664			0.22	0.63	3.95	0.97	0.814	0.542
	B <sub>3</sub>	2.658			0.12	0.25	4.93	0.55	0.756	0.52
	C <sub>1</sub>	2.659	1.6		0.35	1.00	3.06	1.22	0.845	0.562
	C <sub>2</sub>	2.664			0.25	0.63	3.09	1.02	0.856	0.576
	C <sub>3</sub>	2.665			0.11	0.25	4.45	0.63	0.828	0.529
Group 2	D <sub>1</sub>	2.657	4	0.0016	0.302	1.00	4.28	1.2	0.747	0.536
	D <sub>2</sub>	2.650			0.44	1.60	4.43	1.08	0.759	0.586
	D <sub>3</sub>	2.655			0.435	2.50	6.31	1.1	0.694	0.509
	E <sub>1</sub>	2.654		0.25	0.43	1.00	3.12	0.94	0.797	0.561
	E <sub>2</sub>	2.651			0.52	1.60	3.8	0.96	0.807	0.545
	E <sub>3</sub>	2.661			0.68	2.50	4.02	1.05	0.822	0.569
	F <sub>1</sub>	2.664		0.63	0.69	1.00	1.79	0.8	0.844	0.621
	F <sub>2</sub>	2.652			0.78	1.60	2.47	0.88	0.782	0.566
	F <sub>3</sub>	2.660			0.85	2.50	3.2	1.03	0.788	0.574

shows the different samples under study. Their index properties are presented in Table 1. Their grain size distribution curves are shown in Fig. 4. The tested samples were prepared according to their extreme grain sizes ( $D_{max}$  and  $D_{min}$ ) and mean grain sizes ( $D_{50}$ ) and they were subdivided into two groups as the following.

Group 1 includes samples A<sub>i</sub>, B<sub>i</sub> and C<sub>i</sub> ( $1.6 \text{ mm} \leq D_{max} \leq 4.0 \text{ mm}$ ,  $D_{min} = 0.0016 \text{ mm}$  and  $0.25 \text{ mm} \leq D_{50} \leq 1.0 \text{ mm}$ ) and group 2 includes samples D<sub>i</sub>, E<sub>i</sub> and F<sub>i</sub> ( $D_{max} = 4.0 \text{ mm}$ ,  $0.0016 \text{ mm} \leq D_{min} \leq 0.63 \text{ mm}$ , and  $1.0 \text{ mm} \leq D_{50} \leq 2.5 \text{ mm}$ ).

The maximum void ratio ( $e_{max}$ ) corresponding to the loosest state of the soil sample and minimum void ratio ( $e_{min}$ ) corresponding to the densest state of the soil sample were determined according to ASTM D4253 and ASTM D4254 standards for the different samples used in this laboratory investigation.

### 3.2 Effects of $D_{50}$ , $D_{max}$ and $D_{min}$ on $e_{max}$ and $e_{min}$

The effects of the extreme grain sizes ( $D_{max}$  and  $D_{min}$ ) and mean grain size ( $D_{50}$ ) on the generated void ratios (void ratios after consolidation phase) considering the selected initial relative density ( $D_r = 25\%$ ) are presented in Fig. 5. As it can be seen from Fig. 5a, the extreme void

ratios ( $e_{max}$  and  $e_{min}$ ) decrease with the increase of the maximum grain size ( $D_{max}$ ) for the selected mean grains sizes ( $D_{50} = 1, 0.63$  and  $0.25 \text{ mm}$ ). The inverse tendency is observed as the minimum grain size ( $D_{min}$ ) increases ( $0.0016 \text{ mm} \leq D_{min} \leq 0.63 \text{ mm}$ ) for the  $1.00 \text{ mm}$  mean grain size (Fig. 5b). For the  $1.6 \text{ mm}$  mean grain size, the maximum void ratio increases as the minimum grain size increases from  $D_{min} = 0.0016$ – $0.25 \text{ mm}$ , after that it decreases moderately. For the same mean grain size ( $D_{50} = 1.6 \text{ mm}$ ), the minimum void ratio decreases in the range from  $0.0016$  to  $0.25 \text{ mm}$  beyond that it increases slowly. For  $D_{50} = 2.5 \text{ mm}$ , the maximum void ratio increases with the increase of the minimum grain size from  $D_{min} = 0.0016$  to  $0.25 \text{ mm}$  then it decreases until  $D_{min} = 0.63 \text{ mm}$ . However, the minimum void ratio increases with the increase of  $D_{min}$  for the same mean grain size ( $D_{50} = 2.5 \text{ mm}$ )

### 3.3 Sample Preparation

Liquefaction resistance characteristics of silty sand soils depend primarily on the sample preparation techniques and consequently on the arrangement of the particles. Published literature (Ishihara 1993; Vaid et al. 1999 as well as Mahmoudi et al. 2013) has

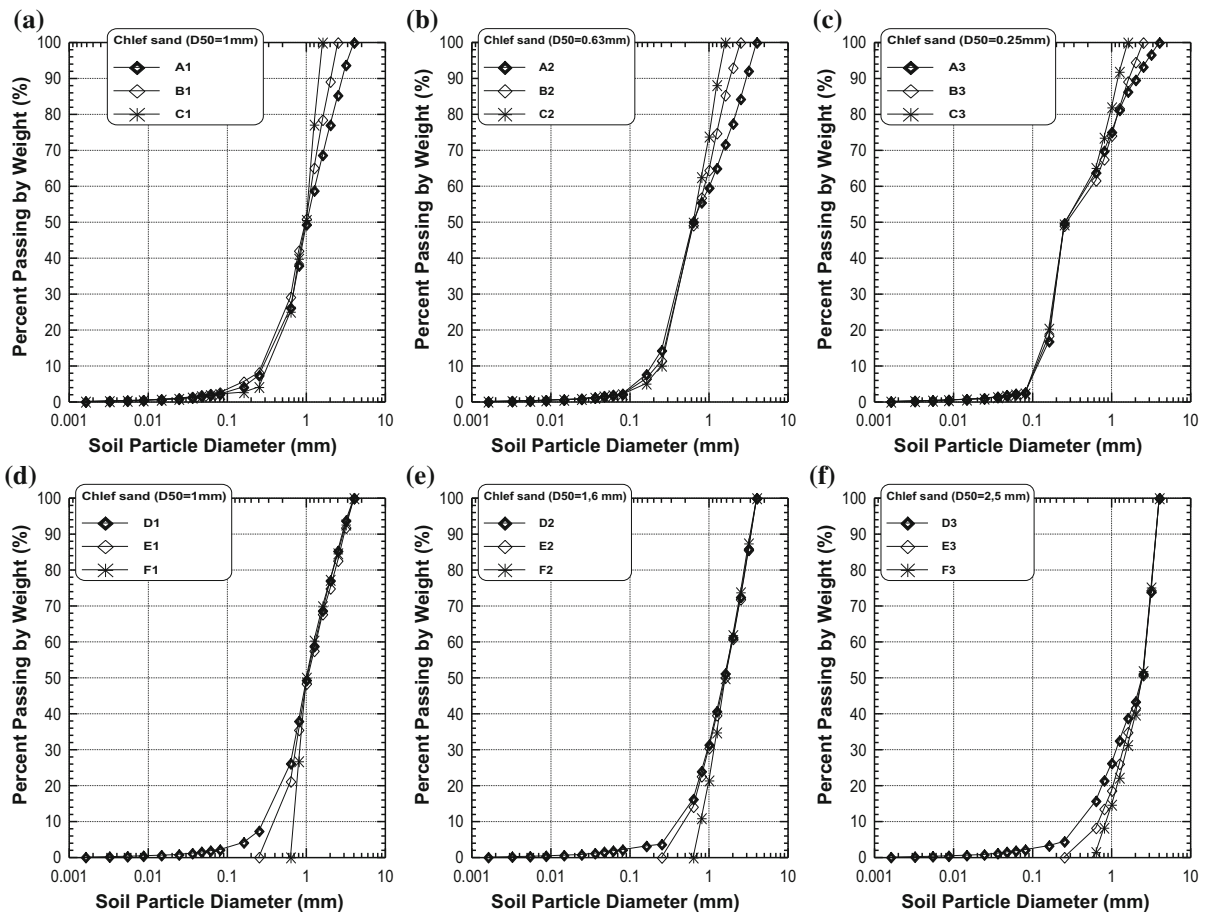


**Fig. 4** Grain size distribution curves of tested materials. **a**  $D_{50} = 1.0$  mm. **b**  $D_{50} = 0.63$  mm. **c**  $D_{50} = 0.25$  mm. **d**  $D_{50} = 1.0$  mm. **e**  $D_{50} = 1.6$  mm. **f**  $D_{50} = 2.5$  mm

systematically discussed the strong impact of sample reconstitution techniques on the liquefaction resistance susceptibility of sand. The main objective of selecting the appropriate one is to reproduce the natural deposit of sands. Since most sandy sites that experienced liquefaction phenomenon under different loading conditions have been deposited under alluvial or marine conditions, a depositional method that replicates these low input energy depositional processes should be selected. Wet deposition or moist tamping as mentioned in the geotechnical engineering published literature by different authors (Vaid et al. 1999; Høeg et al. 2000; Frost and Park 2003; Yamamuro and Wood 2004; Carraro and Prezzi 2008; Sadrekarimi and Olson 2012) has been shown to create a grain structure similar to that of naturally deposited river sands. Mahmoudi et al. (2013) indicated that wet deposition is the most popular

laboratory method to prepare loose sand samples and it consists of placing sand layers of specified thickness into a mold and tamping each layer with a flat tamper. Therefore, it is selected as a suitable sample depositional technique for the present experimental program.

The dry sand was mixed with a water content of  $w = 5\%$ . The samples have been prepared with diameter (D) of 100 mm and height (H) of 200 mm ( $H/D = 2$  was kept constant) using five layers with a constant thickness of 40 mm for each layer. The samples were prepared with the help of a mold composed of two semi-cylindrical shells. In order to maintain the cuff made of latex along the partitions of the mold (Bayat and Bayat 2012), four aspiration ducts are pierced in the conducted shells. These ducts communicate with the inside of the mold by rows of small holes. They are joined to flexible hoses that are assembled in a single tube. This last can be connected to a vacuum pump.

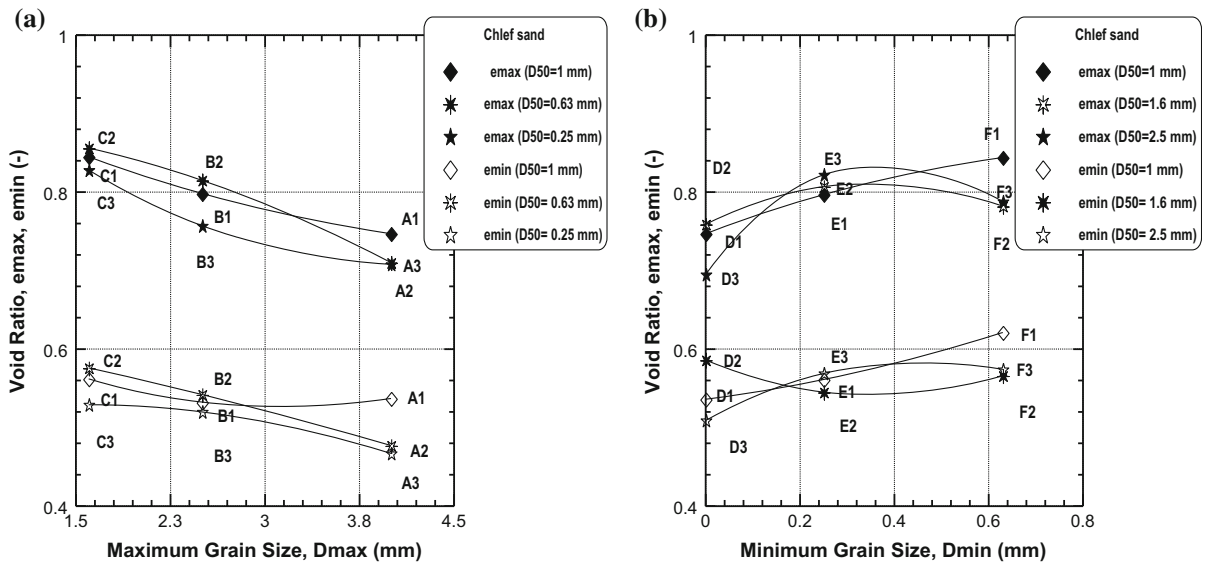


**Fig. 5** Extreme voids ratios index versus extreme grain sizes. **a** Group 1 ( $1.6 \text{ mm} \leq D_{\text{max}} \leq 4.0 \text{ mm}$ ,  $D_{\text{min}} = 0.0016 \text{ mm}$ ,  $0.25 \text{ mm} \leq D_{50} \leq 1.0 \text{ mm}$ ). **b** Group 2 ( $D_{\text{max}} = 4.0 \text{ mm}$ ,  $0.0016 \text{ mm} \leq D_{\text{min}} \leq 0.63 \text{ mm}$ ,  $1.0 \text{ mm} \leq D_{50} \leq 2.5 \text{ mm}$ )

### 3.4 Saturation and Consolidation

The saturation process was done to ensure that all the voids within the test sample were filled with water. The technique of CO<sub>2</sub> suggested by Lade and Duncan (1973) was used to assure a higher degree of saturation. The evaluation of the sample saturation was done by means of Skempton’s pore pressure parameter B through the application of a backpressure of 200 kPa for all tests and a minimum value greater than 0.97 was obtained. After samples were fully saturated, then they were subjected to a constant confining pressure of 100 kPa.

### 3.5 Shear Loading

All undrained monotonic triaxial tests for this study were carried out at a constant strain rate of 0.2 mm per minute, which was slow enough to allow pore pressure change to equalize throughout the sample with the pore pressure measured at the base of sample. All the undrained triaxial tests were continued up to 24% axial strain.

### 3.6 Post-consolidation and Initial Sample Void Ratio Relationship

For the purpose of finding a relationship between the initial void ratio ( $e_i$ ) and post-consolidation void ratio ( $e_c$ ) of the different reconstituted samples (group 1 and group 2) used in this experimental study considering the two

ranges of the selected mean grain sizes ( $0.25 \text{ mm} \leq D_{50} \leq 1.0 \text{ mm}$  and  $1.0 \text{ mm} \leq D_{50} \leq 2.5 \text{ mm}$ ). Figure 6 presents the relationship between the post-consolidation void ratio and the initial void ratio. It is clear that the post-consolidation void ratio decreases with the decrease of the initial void ratio as the mean grain size increases from  $D_{50} = 0.25 \text{ mm}$  to  $D_{50} = 1 \text{ mm}$  for group 1. However, group 2 shows similar void ratio trend as the mean grain size decreases from  $D_{50} = 2.5 \text{ mm}$  to  $D_{50} = 1 \text{ mm}$ . Moreover, It is also observed that group 1 ( $A_i$ ,  $B_i$  and  $C_i$ ) generates higher void ratios range comparing to group 2 generating lower void ratio variations. This can be attributed to the impact of the  $D_{\text{max}}$  parameter for group 1 rather than the effect of  $D_{\text{min}}$  parameter for group 2. The following expression is suggested to relate the post-consolidation void ratio ( $e_c$ ) with the initial void ratio ( $e_i$ ) of the eighteen samples under consideration

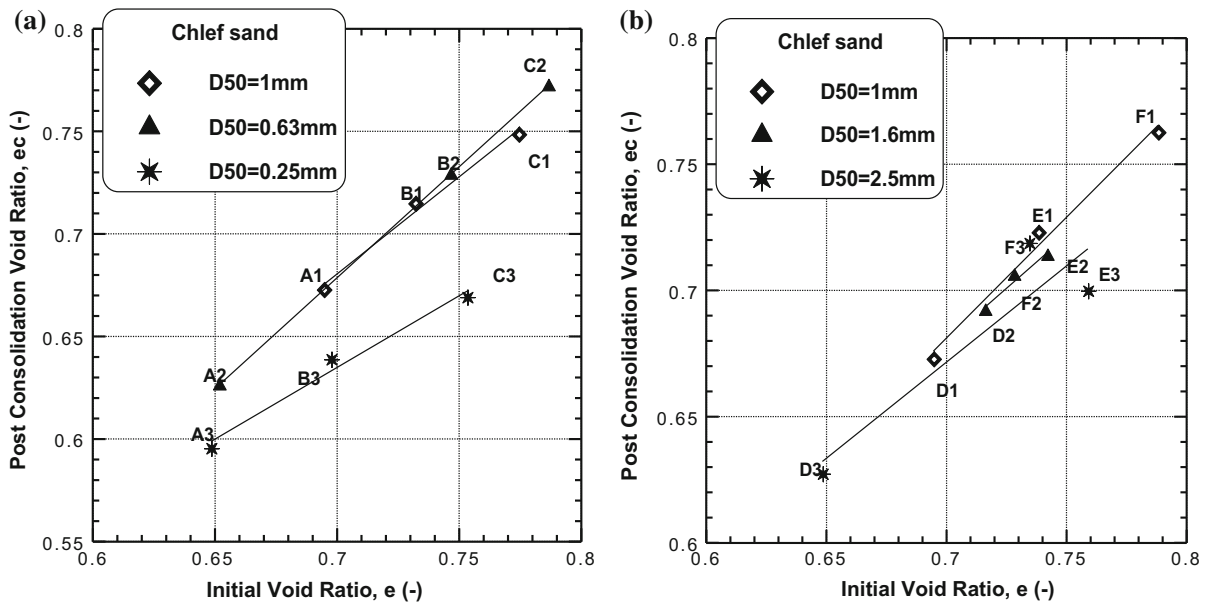
$$(e_c) = a * (e_i) + c \tag{1}$$

Table 2 illustrates the coefficients a, c and the corresponding coefficient of determination ( $R^2$ ) for the selected material under consideration.

### 3.7 Post-consolidation Void Ratio and Mean Grain Size Relationship

Figure 7 shows the variation of the generated post consolidation void ratio with the mean grain size ( $D_{50}$ )





**Fig. 6** Post-consolidation void ratio versus initial void ratio ( $D_r = 25\%$ ,  $P'_c = 100$  kPa). **a** Group 1 ( $1.6 \text{ mm} \leq D_{\max} \leq 4.0 \text{ mm}$ ,  $D_{\min} = 0.0016 \text{ mm}$ ,  $0.25 \text{ mm} \leq D_{50} \leq 1.0 \text{ mm}$ ).

**b** Group 2 ( $D_{\max} = 4.0 \text{ mm}$ ,  $0.0016 \text{ mm} \leq D_{\min} \leq 0.63 \text{ mm}$ ,  $1.0 \text{ mm} \leq D_{50} \leq 2.5 \text{ mm}$ )

**Table 2** Coefficients a, c and  $R^2$  for Eq. (1)

Extreme sizes	$D_{50}$ (mm)	a	c	$R^2$
Group 1 ( $A_i$ , $B_i$ and $C_i$ )	1.00	0.94	0.01	0.99
$1.6 \text{ mm} \leq D_{\max} \leq 4 \text{ mm}$	0.63	1.08	-0.07	0.99
$D_{\min} = 0.0016 \text{ mm}$	0.25	0.69	0.14	0.98
Group 2 ( $D_i$ , $E_i$ and $F_i$ )	1.00	0.95	0.01	0.99
$D_{\max} = 4.0 \text{ mm}$	1.60	0.83	0.09	0.96
$0.0016 \text{ mm} \leq D_{\min} \leq 0.63 \text{ mm}$	2.50	0.76	0.13	0.84

of the tested wet deposited samples ( $e_c$ ) reconstituted at an initial relative density ( $D_r = 25\%$ ) for two ranges of the extreme grain sizes ( $1.6 \text{ mm} \leq D_{\max} \leq 4.0 \text{ mm}$  and  $0.0016 \text{ mm} \leq D_{\min} \leq 0.63 \text{ mm}$ ). It is observed from Fig. 7 that the overall soil sample trend exhibits a decrease of the post consolidation void ratio with the increase of the mean grain size ( $D_{50}$ ) for samples of group 01 and 02 and they display a meaningful linear relationship for the initial relative density under study. The obtained data indicate that the lower mean grain sizes exhibit higher void ratios for a given extreme grain sizes ( $D_{\max}$  and  $D_{\min}$ ).

The effect of the extreme grain sizes ( $D_{\max}$  and  $D_{\min}$ ) on the generated void ratios of different soil particle packings ( $e_c$ ) is clearly observed for higher mean grain sizes and becomes very pronounced for

lower mean grain sizes. The post-consolidation void ratio could be related to the mean grain size through the following relation:

$$(e_c) = a * (D_{50}) + c \tag{2}$$

Table 3 illustrates the coefficients a, c and the corresponding coefficient of determination ( $R^2$ ) for the selected material under consideration.

#### 4 Monotonic Triaxial Compression Test Results

Figures 8, 9, 10, 11, 12 and 13 illustrate the undrained monotonic compression triaxial test results of eighteen sandy samples classified into two groups ( $A_i$ ,  $B_i$ ,  $C_i$ ) and ( $D_i$ ,  $E_i$ ,  $F_i$ ) prepared in laboratory with different

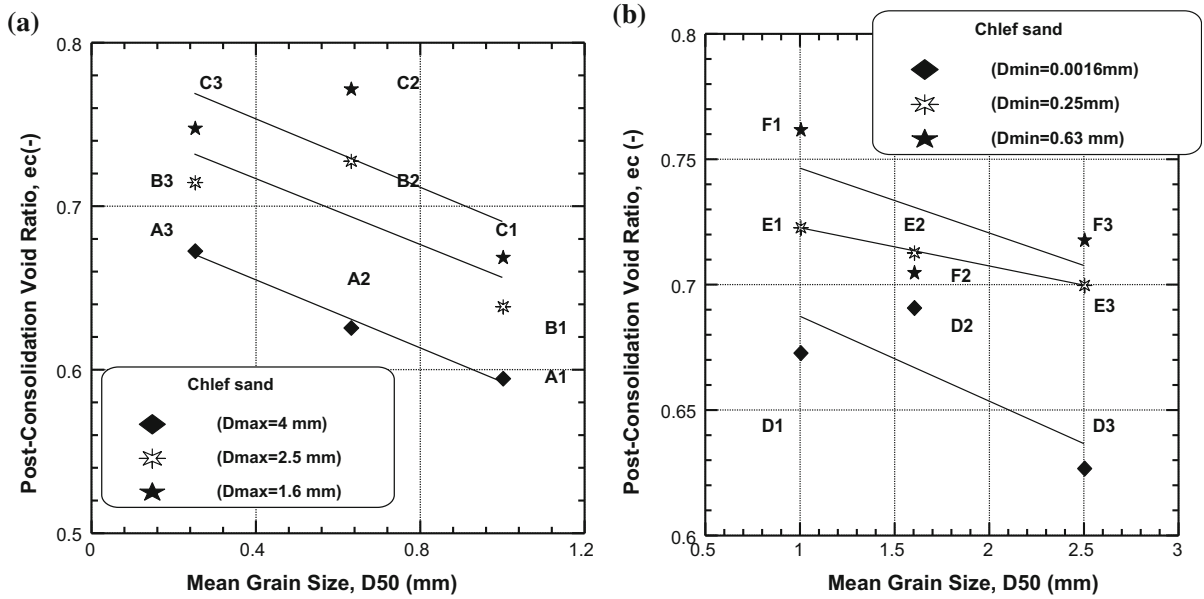


**Fig. 7** Post-consolidation void ratio versus mean grain size ( $D_r = 25\%$ ,  $P'_c = 100$  kPa). **a** Group 1 ( $1.6 \text{ mm} \leq D_{\max} \leq 4.0 \text{ mm}$ ,  $D_{\min} = 0.0016 \text{ mm}$ ). **b** Group 2 ( $D_{\max} = 4.0 \text{ mm}$ ,  $0.0016 \text{ mm} \leq D_{\min} \leq 0.63 \text{ mm}$ )

**Table 3** Coefficients  $a$ ,  $c$  and  $R^2$  for Eq. (2)

Extreme sizes	$D_{\max}$ or $D_{\min}$ (mm)	$a$	$c$	$R^2$
Group 1 ( $A_i$ , $B_i$ and $C_i$ )	4.0	-0.10	0.69	0.98
$1.6 \text{ mm} \leq D_{\max} \leq 4.0 \text{ mm}$	2.5	-0.10	4.75	0.62
$D_{\min} = 0.0016 \text{ mm}$	1.6	-0.10	0.80	0.53
Group 2 ( $D_i$ , $E_i$ and $F_i$ )	0.0016	-0.03	0.72	0.60
$D_{\max} = 4.0 \text{ mm}$	0.25	-0.01	0.74	0.99
$0.0016 \text{ mm} \leq D_{\min} \leq 0.63 \text{ mm}$	0.63	-0.02	0.77	0.43

mean grain sizes ranging between  $D_{50} = 0.25 \text{ mm}$  and  $D_{50} = 1 \text{ mm}$  for group 01 and from  $D_{50} = 1 \text{ mm}$  to  $D_{50} = 2.5 \text{ mm}$  for group 02. All the samples were reconstituted at an initial relative density ( $D_r = 25\%$ ) and subjected to a constant confining pressure ( $P'_c = 100 \text{ kPa}$ ). It can be observed from Figs. 8, 9, 10, 11, 12 and 13 that complete static liquefaction cases were recorded for the different samples of group 01 and 02 with a clear impact of the extreme size parameters ( $D_{\max}$  and  $D_{\min}$ ) and the mean grain size parameter ( $D_{50}$ ) on the undrained shear strength (liquefaction resistance) response. Figures 8a and 9a illustrate clearly that the undrained shear strength of  $A_i$  samples ( $q_{\max} = 70.94 \text{ kPa}$  for  $A_1$ ,  $q_{\max} = 56.18 \text{ kPa}$  for  $A_2$  and  $q_{\max} = 43.97 \text{ kPa}$  for  $A_3$ ) and  $B_i$  samples ( $q_{\max} = 67.97 \text{ kPa}$  for  $B_1$ ,  $q_{\max} = 58.19 \text{ kPa}$  for  $B_2$

and  $q_{\max} = 43.42 \text{ kPa}$  for  $B_3$ ) decreases with the decrease of the mean grain size ranging from  $D_{50} = 1 \text{ mm}$  to  $D_{50} = 0.25 \text{ mm}$ . However a slight increase then a decrease in the undrained shear strength (Fig. 10a) has been recorded for  $C_i$  samples ( $q_{\max} = 64.33 \text{ kPa}$  for  $C_1$ ,  $q_{\max} = 68.71 \text{ kPa}$  for  $C_2$  and  $q_{\max} = 42.51 \text{ kPa}$  for  $C_3$ ). It is observed that the higher  $D_{\max}$  and  $D_{50}$ , the higher undrained shear strength for  $A_i$  and  $B_i$  samples. This outcome results from the combined effect of  $D_{\max}$  and  $D_{50}$  parameters in increasing the undrained shear strength due to the interlocking of coarse grained with fine grained and the dilation phase amplification leading to a more stable structures of the soil samples at 1.5% axial strain. Beyond that, all the samples of group 01 exhibit flow behaviour and the steady state has been reached

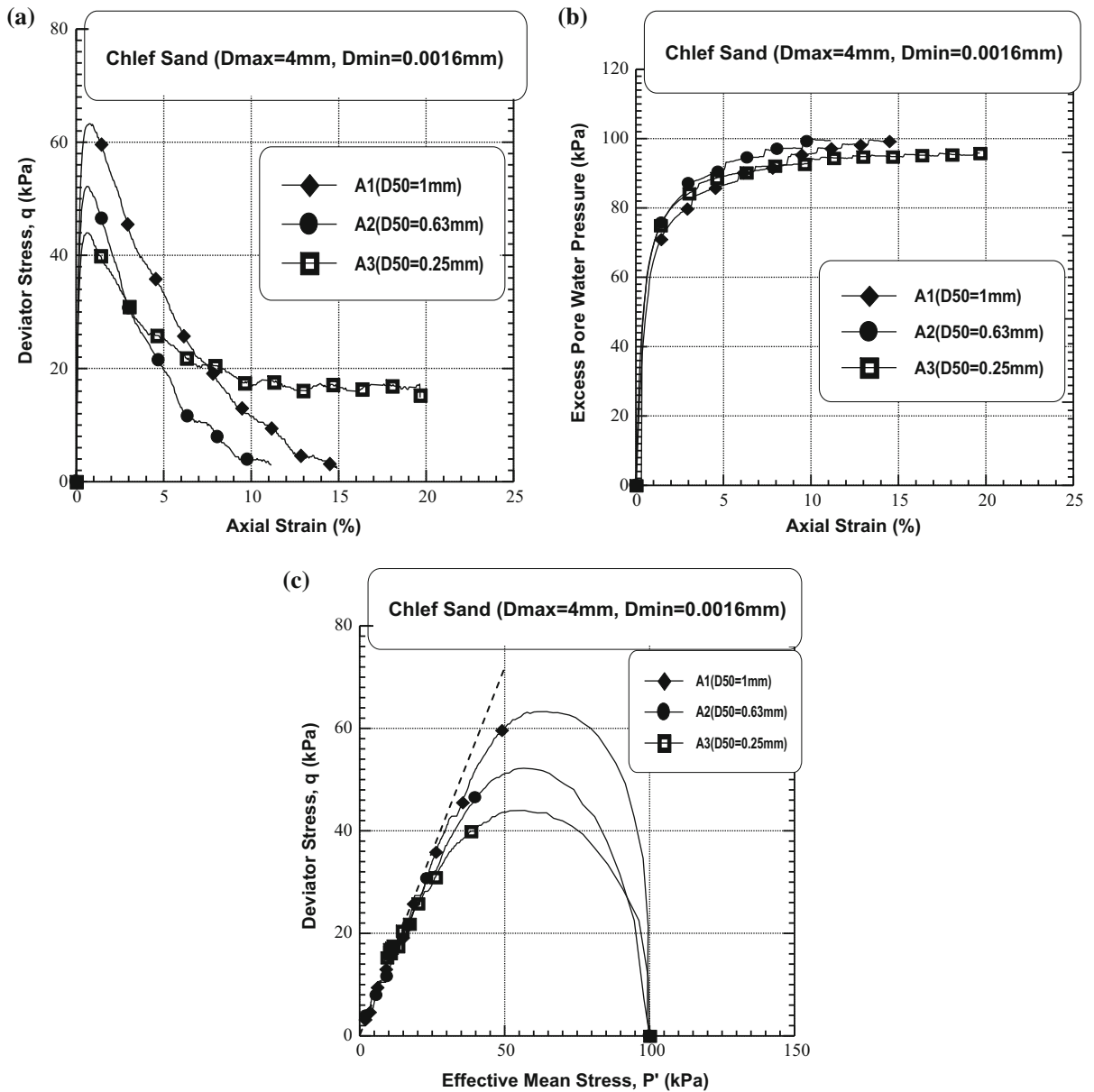


**Fig. 8** Undrained monotonic behavior of Chlef sand ( $A_i$  samples) ( $D_{max} = 4.0$  mm,  $D_{min} = 0.0016$  mm,  $0.25$  mm  $\leq D_{50} \leq 1.0$  mm,  $D_r = 25\%$ ,  $P'_c = 100$  kPa). **a** Deviator stress

versus axial strain. **b** Excess Pore Pressure versus axial strain. **c** Deviator stress versus Effective mean Stress

within 15–20% axial strain. All the samples of group 01 ( $A_i$ ,  $B_i$  and  $C_i$ ) exhibit flow behaviour (Fig. 11b). The inverse tendency was observed for the  $D_i$  ( $q_{max} = 70.94$  kPa for  $D_1$ ,  $q_{max} = 70.78$  kPa for  $D_2$  and  $q_{max} = 81.81$  kPa for  $D_3$ ) and  $E_i$  ( $q_{max} = 66.88$  kPa for  $E_1$ ,  $q_{max} = 69.90$  kPa for  $E_2$  and  $q_{max} = 69.95$  kPa for  $E_3$ ) samples (group 02), where the undrained shear strength increases with the

increase of the mean grain size from  $D_{50} = 1$  mm to 2.5 mm. The  $D_i$  and  $E_i$  present flow behaviour ( $D_1$  and  $E_1$ ) and limited flow behaviour ( $D_2$ ,  $D_3$ ,  $E_2$  and  $E_3$ ). For  $F_i$  samples (Fig. 13a), a moderate decrease followed by a significant increase in the undrained shear strength was observed ( $q_{max} = 88.93$  kPa for  $F_1$ ,  $q_{max} = 83.02$  kPa for  $F_2$  and  $q_{max} = 133.27$  kPa for  $F_3$ ) at an average axial strain of 2%. Beyond that, the  $F_i$

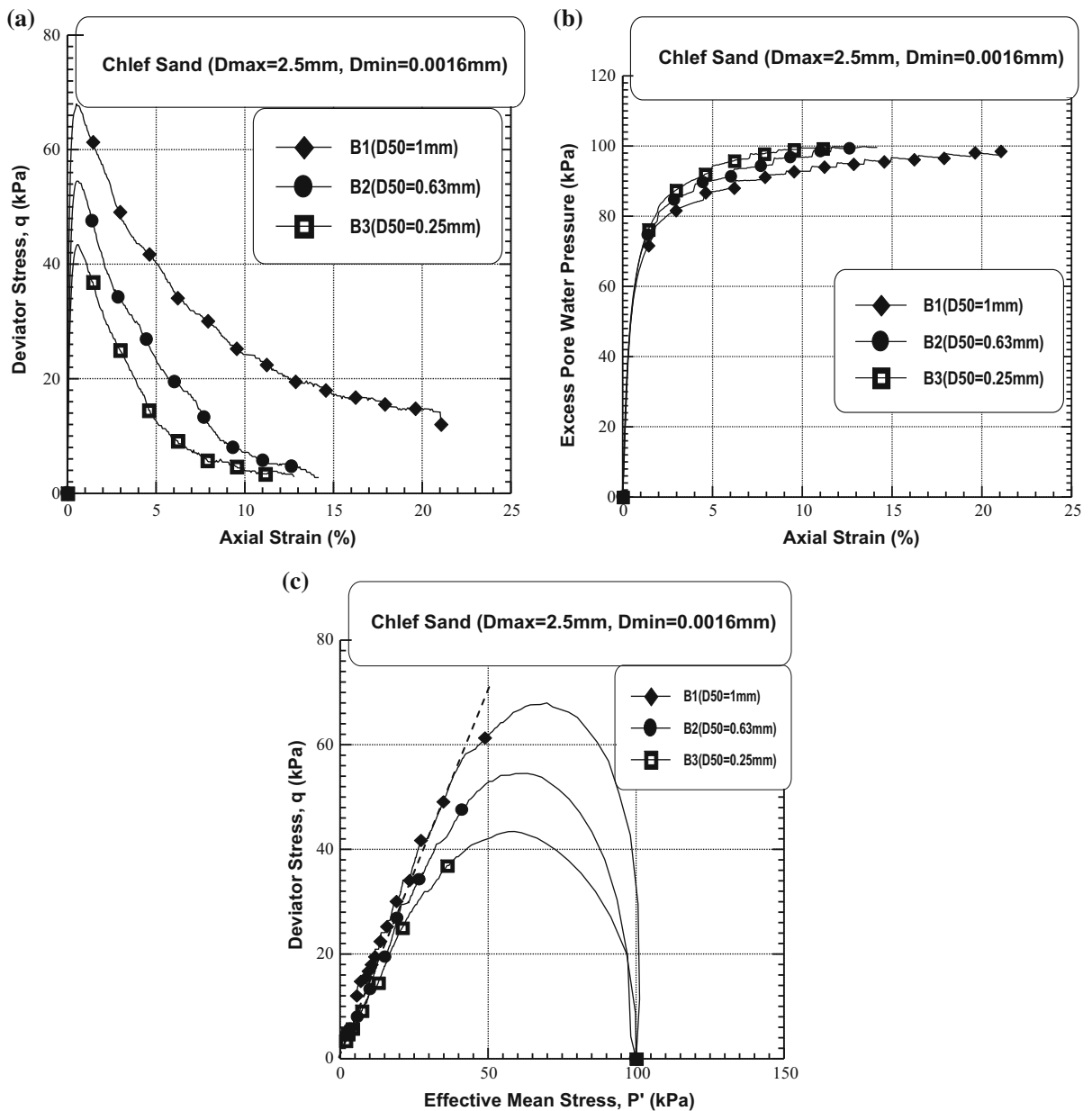


**Fig. 9** Undrained monotonic behavior of Chlef sand (B<sub>i</sub> samples) (D<sub>max</sub> = 2.5 mm, D<sub>min</sub> = 0.0016 mm, 0.25 mm ≤ D<sub>50</sub> ≤ 1.0 mm, D<sub>r</sub> = 25%, P'<sub>c</sub> = 100 kPa). **a** Deviator stress versus

axial strain. **b** Excess Pore Pressure versus axial strain. **c** Deviator stress versus Effective mean Stress

samples exhibit limited flow, flow and non flow behaviour respectively for F<sub>1</sub>, F<sub>2</sub> and F<sub>3</sub> (Fig. 13a) respectively for F<sub>1</sub>, F<sub>2</sub> and F<sub>3</sub>. The outcome of the present study is in good agreement with the experimental work reported by Yilmaz and Mollamahmutoglu (2009) and Belkhatir et al. (2014). Figures 8b, 9b, 10b, 11b, 12b and 13b show the excess pore water

pressure versus axial strain. It can be seen that the excess pore water pressure increases with the decrease of mean grain size from D<sub>50</sub> = 1.0 mm to 0.25 mm for 1.6 mm ≤ D<sub>max</sub> ≤ 4 mm and from D<sub>50</sub> = 2.5 mm to 1 mm for 0.0016 mm ≤ D<sub>min</sub> ≤ 0.63 mm. The stress path in the (p', q) plane shows clearly the role of the extreme sizes and mean grain size to decrease the

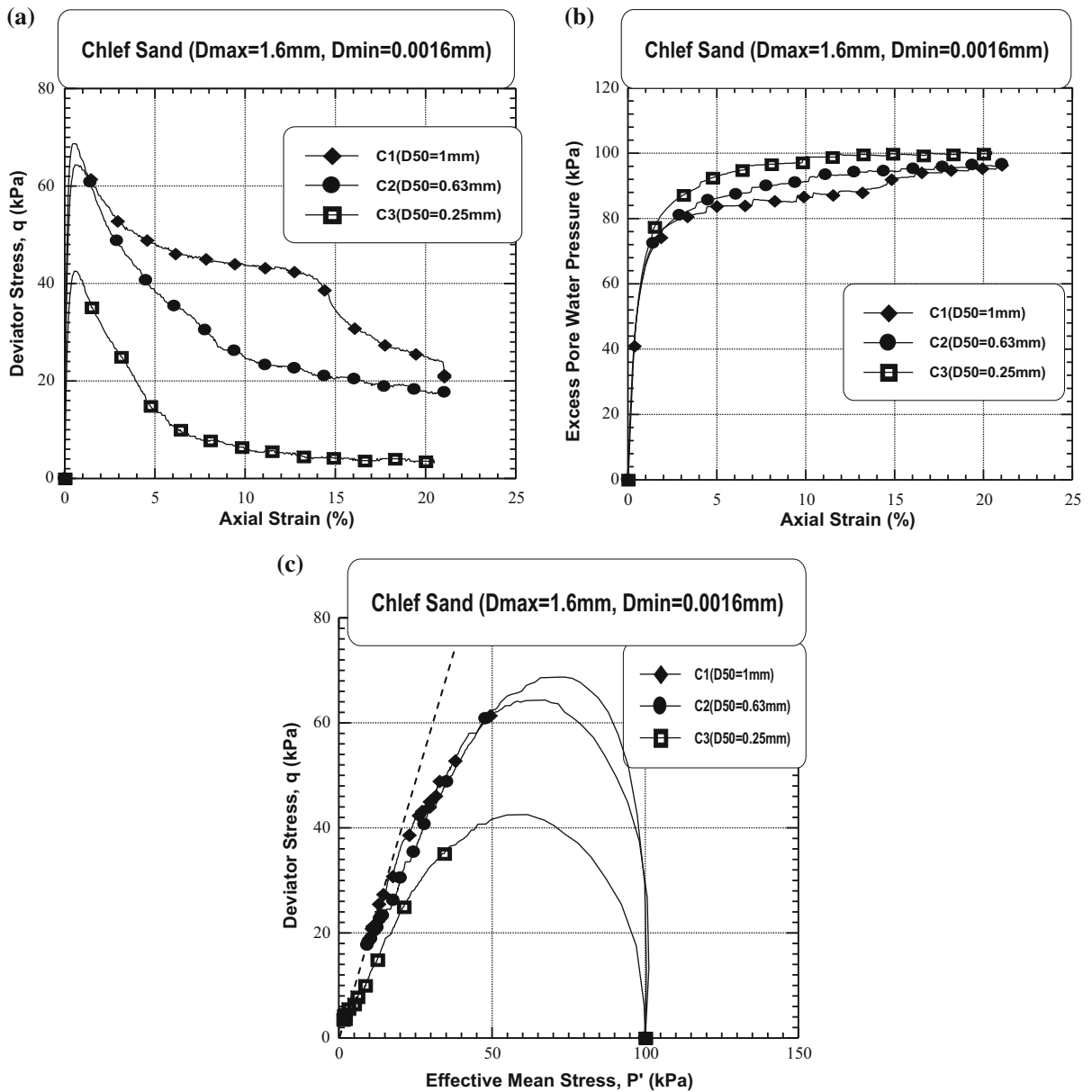


**Fig. 10** Undrained monotonic behavior of Chlef sand ( $C_i$  samples) ( $D_{max} = 1.6 \text{ mm}$ ,  $D_{min} = 0.0016 \text{ mm}$ ,  $0.25 \text{ mm} \leq D_{50} \leq 1 \text{ mm}$ ,  $D_r = 25\%$ ;  $P'_c = 100 \text{ kPa}$ ). **a** Deviator stress

versus axial strain. **b** Excess Pore Pressure versus axial strain. **c** Deviator stress versus Effective mean Stress

average effective pressure and the maximum deviatoric stress (Figs. 8c, 9c, 10c, 11c, 12c, 13c). The influence of the mean grain size ( $D_{50}$ ) and extreme sizes ( $D_{max}$  and  $D_{min}$ ) parameters on the generated excess pore water pressure is clearly observed for the samples of group 02 ( $D_i$ ,  $E_i$  and  $F_i$ ) and becomes very pronounced for group 1 ( $A_i$ ,  $B_i$  and  $C_i$ ).

Tables 4 and 5 present a summary of the undrained monotonic triaxial compression tests respectively for group 1 and group 2).

Figure 14 illustrates the view of two samples after shearing: Fig. 14a shows the sample  $F_3$  ( $D_{50} = 2.5 \text{ mm}$ ,  $ec = 0.718$ ,  $D_{max} = 4 \text{ mm}$ ,  $D_{min} = 0.0016 \text{ mm}$ ) exhibiting non flow behavior



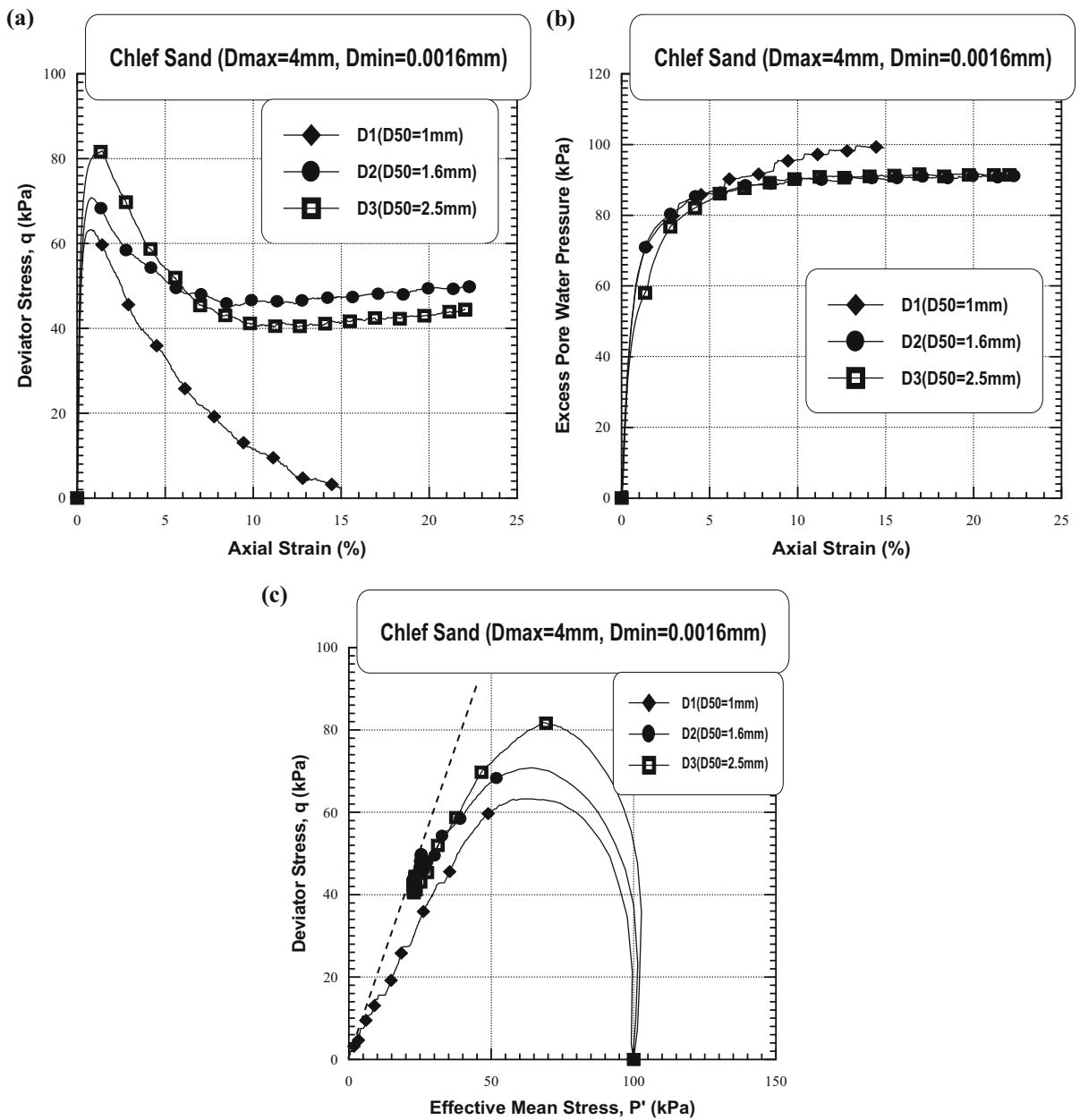


**Fig. 11** Undrained monotonic behavior of Chlef sand ( $D_i$  samples) ( $D_{max} = 4\text{ mm}$ ,  $D_{min} = 0.0016\text{ mm}$ ,  $1.0\text{ mm} \leq D_{50} \leq 2.5\text{ mm}$ ,  $D_r = 25\%$ ,  $P'_c=100\text{ kPa}$ ). **a** Deviator stress versus

axial strain. **b** Excess Pore Pressure versus axial strain. **c** Deviator stress versus Effective mean Stress

and dilation phenomena. The contrary was observed for the case of the sample  $A_2$  ( $D_{50} = 0.63\text{ mm}$ ,  $ec = 0.626$ ,  $D_{max} = 4\text{ mm}$ ,  $D_{min} = 0.0016\text{ mm}$ ), where flow behavior (complete liquefaction) was observed at the end of the shearing (Fig. 14b).

### 5 Relationship Between Extreme Grain Sizes and Post-consolidation Void Ratio

The effects of the maximum grain size ( $D_{max}$ ) and minimum grain size ( $D_{min}$ ) on the generated sand void

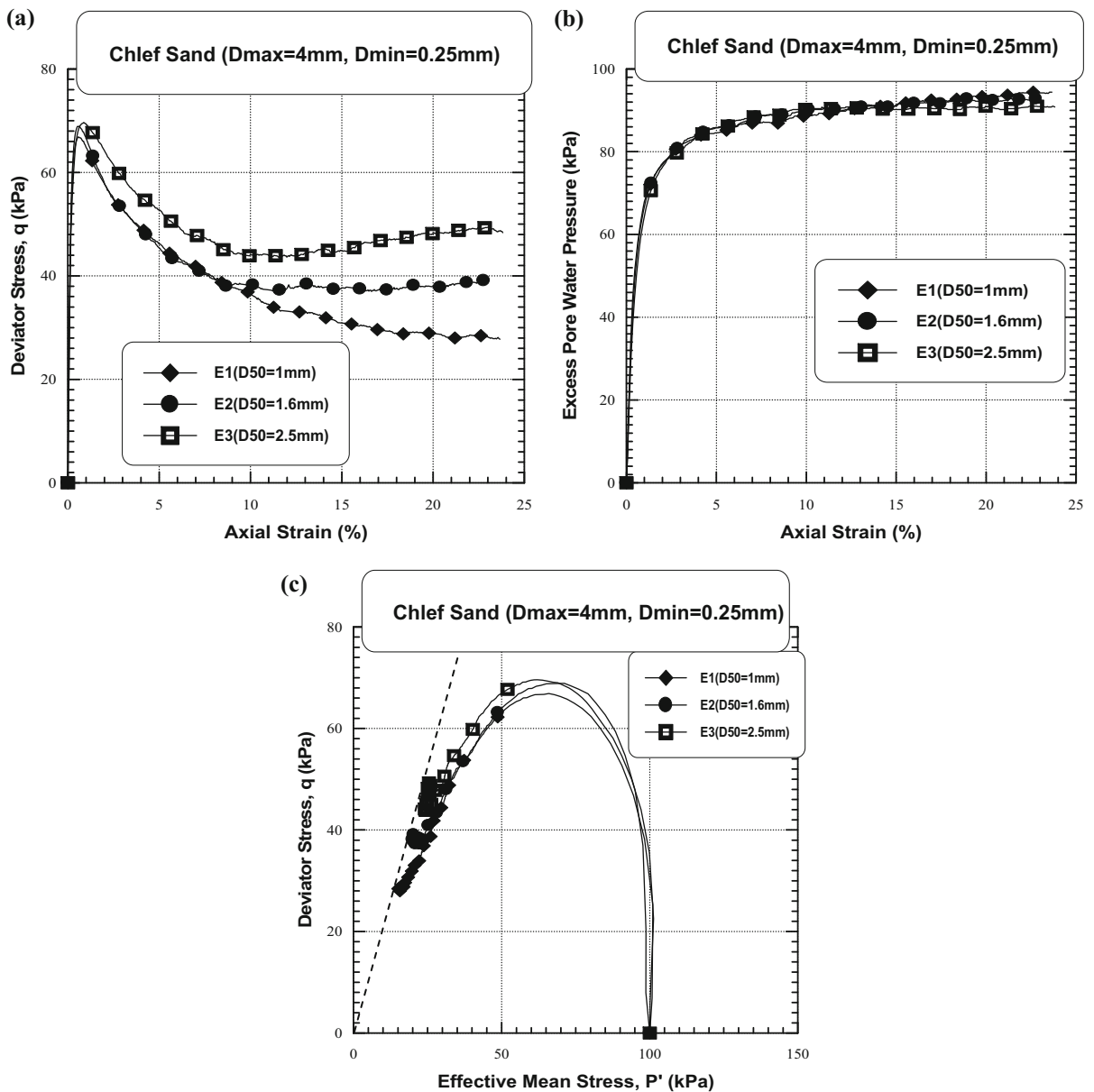


**Fig. 12** Undrained monotonic behavior of Chlef sand ( $E_i$  samples) ( $D_{max} = 4$  mm,  $D_{min} = 0.25$  mm,  $1.0$  mm  $\leq D_{50} \leq 2.5$  mm,  $D_r = 25\%$ ,  $P'_c = 100$  kPa). **a** Deviator stress versus

axial strain. **b** Excess Pore Pressure versus axial strain. **c** Deviator stress versus Effective mean Stress

ratio (void ratio after consolidation phase) considering two mean grain size ranges ( $0.25$  mm  $\leq D_{50} \leq 1$  mm) and ( $1.0$  mm  $\leq D_{50} \leq 2.5$  mm) for the selected initial relative density ( $D_r = 25\%$ ) are presented in Fig. 15. As it can be seen from this plot, the extreme grain sizes ( $D_{max}$  and  $D_{min}$ ) and mean grain size ( $D_{50}$ ) induce a logarithmic decrease of the post-

consolidation void ratio ( $e_c$ ) as the maximum grain size increases from  $D_{max} = 1.6$  mm to  $D_{max} = 4.0$  mm for the selected mean grain size range ( $0.25$  mm  $\leq D_{50} \leq 1.0$  mm) (group 01) and a logarithmic increase of the post-consolidation void ratio ( $e_c$ ) as the minimum grain size increases from  $D_{min} = 0.0016$  mm to  $D_{min} = 0.63$  mm for the

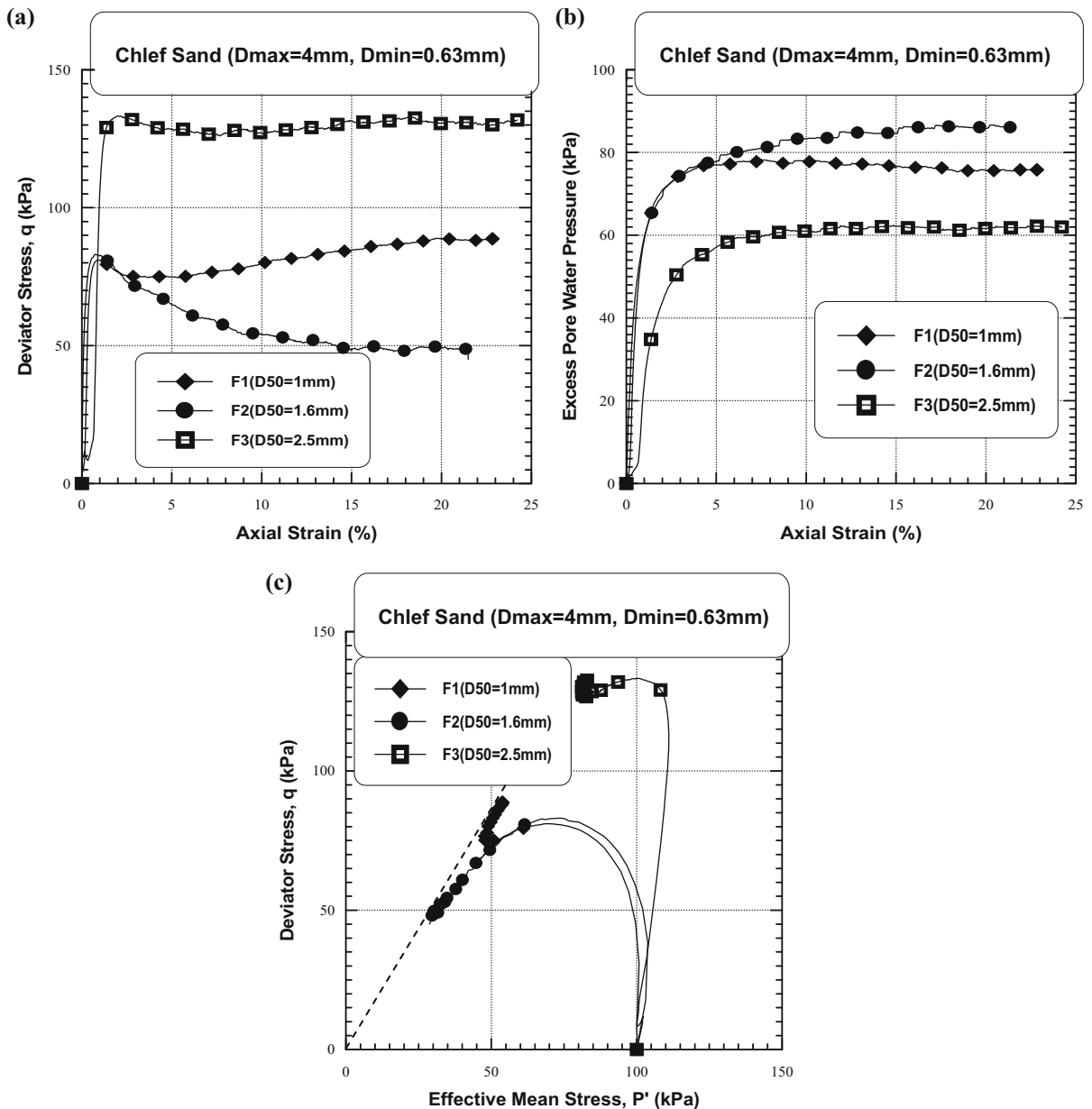


**Fig. 13** Undrained monotonic behavior of Chlef sand ( $F_i$  samples) ( $D_{\max} = 4$  mm,  $D_{\min} = 0.63$  mm,  $1.0$  mm  $\leq D_{50} \leq 2.5$  mm,  $D_r = 25\%$ ,  $P'_c = 100$  kPa). **a** Deviator stress versus

axial strain. **b** Excess Pore Pressure versus axial strain. **c** Deviator stress versus Effective mean Stress

selected mean grain size range ( $1.0$  mm  $\leq D_{50} \leq 2.5$  mm) (group 2). The observed post-consolidation void ratio trend can be attributed to the role of the extreme grain size and mean grain size parameters in increasing or decreasing the inter-particle contact as the maximum grain size and minimum grain size increase respectively for group 1 and group 2.

Moreover, it is clearly observed from Fig. 15 that soil samples with lower  $D_{\max}$  exhibit higher void ratios and soil samples with higher  $D_{\max}$  exhibit lower void ratios (Fig. 15a). The inverse tendency of the post-consolidation void ratio is observed in the case of the variation of the minimum grain size ( $D_{\min}$ ) (Fig. 15b). The following expression is suggested to express the

**Table 4** Summary of monotonic triaxial tests for group 1

Characteristics of materials	A <sub>1</sub>	A <sub>2</sub>	A <sub>3</sub>	B <sub>1</sub>	B <sub>2</sub>	B <sub>3</sub>	C <sub>1</sub>	C <sub>2</sub>	C <sub>3</sub>
q <sub>max</sub> (kPa)	70.94	56.18	43.97	67.97	58.19	43.42	64.33	68.71	42.51
Δu <sub>max</sub> (kPa)	99.60	99.80	95.8	98.7	99.40	99.20	96.4	96.8	98.40
e <sub>i</sub> (–)	0.694	0.651	0.648	0.731	0.746	0.697	0.774	0.786	0.753
e <sub>c</sub> (–)	0.673	0.626	0.595	0.715	0.728	0.639	0.748	0.772	0.669
Δe <sub>c</sub> (–)	0.021	0.025	0.052	0.016	0.017	0.058	0.025	0.014	0.083
Soil response	All the samples exhibit flow behaviour								

**Table 5** Summary of monotonic triaxial tests for group 2

Characteristics of materials	D <sub>1</sub>	D <sub>2</sub>	D <sub>3</sub>	E <sub>1</sub>	E <sub>2</sub>	E <sub>3</sub>	F <sub>1</sub>	F <sub>2</sub>	F <sub>3</sub>
q <sub>max</sub> (kPa)	70.94	70.78	81.81	66.88	68.90	69.95	88.93	83.02	133.27
Δu <sub>max</sub> (kPa)	99.60	91.20	91.60	94.40	93	91	78.40	86.60	62.40
e <sub>i</sub> (–)	0.694	0.715	0.648	0.738	0.740	0.758	0.788	0.727	0.734
e <sub>c</sub> (–)	0.673	0.691	0.627	0.723	0.713	0.700	0.762	0.705	0.718
Δe <sub>c</sub> (–)	0.021	0.023	0.020	0.015	0.028	0.058	0.025	0.022	0.015
Soil response	Flow	Limited flow		Flow	Limited flow		Limited flow	Flow	Non flow

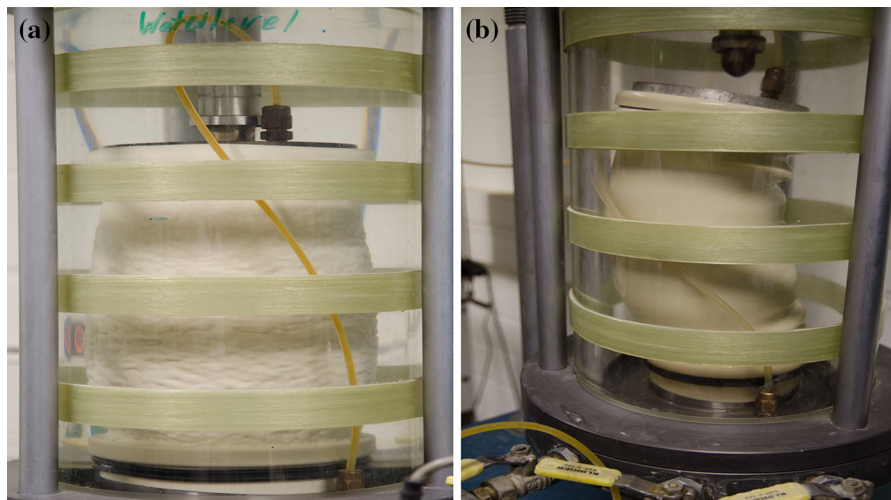


**Fig. 14** View of samples after shearing ( $D_r = 25\%$ ,  $P'_c=100$  kPa). **a** Sample F<sub>3</sub> ( $D_{50} = 2.5$  mm,  $e_c = 0.718$ ) exhibiting non flow behavior. **b** Sample A<sub>2</sub> ( $D_{50} = 0.63$  mm,  $e_c = 0.626$ ) exhibiting flow behavior

post-consolidation void ratio ( $e_c$ ) as a function of the extreme grain sizes ( $D_{max}$ ,  $D_{min}$ ) for the eighteen samples under study:

$$\text{Log}(e_c) = a * \text{log}(D_{max}, D_{min}) + c \tag{3}$$

Table 6 illustrates the coefficients a, c and the corresponding coefficient of determination ( $R^2$ ) for the selected material under consideration.

### 6 Effects of $D_{max}$ and $D_{min}$ on the Maximum Undrained Shear Strength

Data from the present study (Figs. 8, 9, 10, 11, 12, 13) are reproduced in Fig. 16 for the purpose of analyzing the effects of the extreme grain sizes ( $D_{max}$  and  $D_{min}$ ) on the maximum undrained shear strength ( $q_{max}$ ) of eighteen Chlef sand samples for the two selected mean

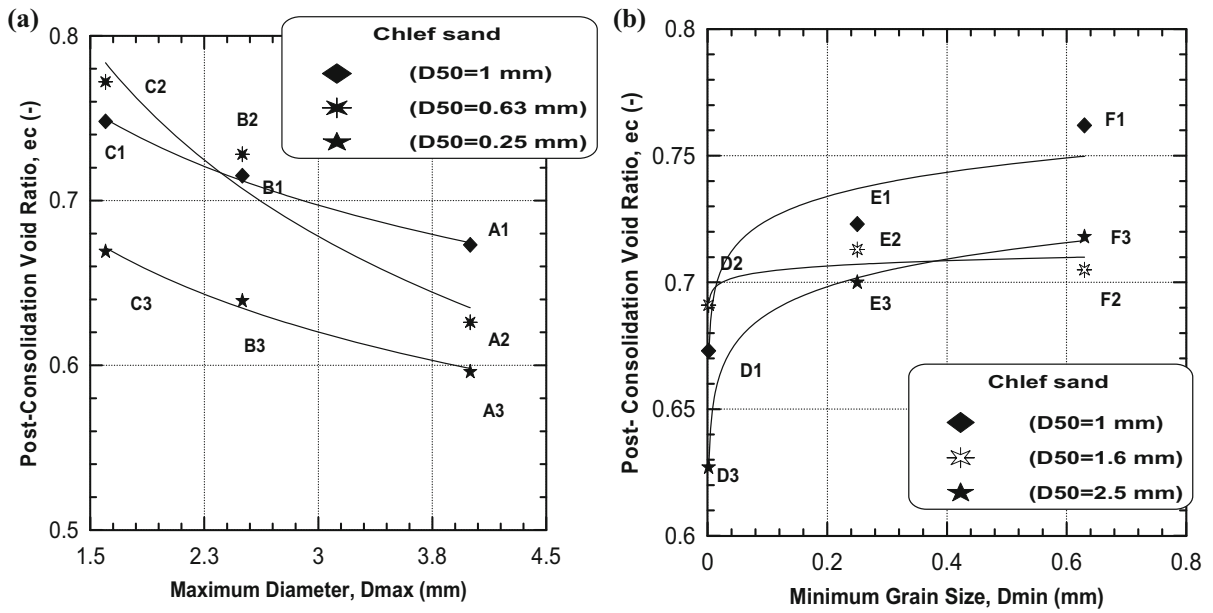


**Fig. 15** Post-consolidation void ratio versus extreme grain sizes ( $D_r = 25\%$ ,  $P'_c = 100$  kPa). **a** Group 1 ( $1.6 \text{ mm} \leq D_{\max} \leq 4.0 \text{ mm}$ ,  $0.25 \text{ mm} \leq D_{50} \leq 1.0 \text{ mm}$ ). **b** Group 2 ( $0.0016 \text{ mm} \leq D_{\min} \leq 0.63 \text{ mm}$ ,  $1.0 \text{ mm} \leq D_{50} \leq 2.5 \text{ mm}$ )

**Table 6** Coefficients  $a$ ,  $c$  and  $R^2$  for Eq. (3)

Extreme sizes	$D_{50}$ (mm)	A	C	$R^2$
Group 1 ( $A_i$ , $B_i$ and $C_i$ )	1.0	-0.11	-0.23	0.99
$1.6 \text{ mm} \leq D_{\max} \leq 4.0 \text{ mm}$	0.63	-0.22	-0.13	0.97
$D_{\min} = 0.0016 \text{ mm}$	0.25	0.12	-0.33	0.99
Group 2 ( $D_i$ , $E_i$ and $F_i$ )	1.0	0.01	0.27	0.92
$D_{\max} = 4.0 \text{ mm}$	1.6	0.004	0.34	0.76
$0.0016 \text{ mm} \leq D_{\min} \leq 0.63 \text{ mm}$	2.5	0.02	-0.32	0.99

grain size ranges ( $0.25 \text{ mm} \leq D_{50} \leq 1.0 \text{ mm}$ ,  $1.0 \text{ mm} \leq D_{50} \leq 2.5 \text{ mm}$ ) and the initial relative density ( $D_r = 25\%$ ) under consideration. It is clearly observed from Fig. 16 that the extreme grain sizes ( $D_{\max}$  and  $D_{\min}$ ) and mean grain size ( $D_{50}$ ) affect significantly the undrained shear strength. The higher and lower mean grain sizes ( $D_{50} = 1.0 \text{ mm}$ ,  $D_{50} = 0.25 \text{ mm}$ ) exhibit a decrease of the maximum undrained shear strength with the decrease of the maximum grain size ( $D_{\max}$ ), while the intermediate mean grain size ( $D_{50} = 0.63 \text{ mm}$ ) shows the inverse soil trend for group 01 (Fig. 16a). This can be attributed to the grain size distribution of  $A_1$ ,  $B_1$  and  $C_1$  and  $A_3$ ,  $B_3$  and  $C_3$  to increase the interlocking and consequently the increase of the undrained shear strength with the increase the maximum grain size

( $D_{\max}$ ) while the grain size distribution of  $A_2$ ,  $B_2$  and  $C_2$  exhibit a decrease of the interlocking and consequently a decrease of the undrained shear strength with the increase the maximum grain size. For group 02, the variation of the mean grain size ( $1.0 \text{ mm} \leq D_{50} \leq 2.5 \text{ mm}$ ) induces an increase of the maximum undrained shear strength with the increase of the minimum grain size ( $D_{\min}$ ). The lower and intermediate mean grain sizes ( $D_{50} = 1.0 \text{ mm}$ ,  $D_{50} = 1.6 \text{ mm}$ ) show a moderate increase of the undrained shear strength, but, the higher mean grain size ( $D_{50} = 2.5 \text{ mm}$ ) exhibits a pronounced increase of the undrained shear strength with the increase of the minimum grain size ( $D_{\min}$ ) (Fig. 16b). The following equations are suggested to express the maximum shear strength ( $q_{\max}$ ) as a function of the maximum and



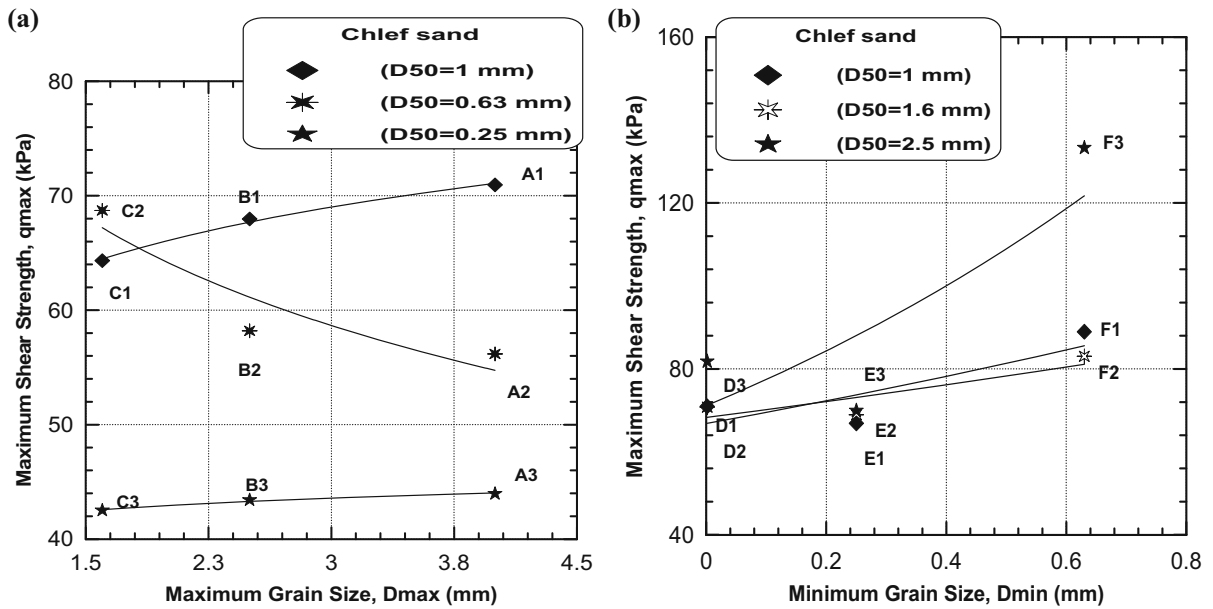


**Fig. 16** Maximum undrained shear strength versus extreme grain sizes ( $D_r = 25\%$ ,  $P'_c = 100$  kPa). **a** Group 1 ( $1.6 \text{ mm} \leq D_{\max} \leq 4.0 \text{ mm}$ ,  $0.25 \text{ mm} \leq D_{50} \leq 1.0 \text{ mm}$ ). **b** Group 2 ( $0.0016 \text{ mm} \leq D_{\min} \leq 0.63 \text{ mm}$ ,  $1.0 \text{ mm} \leq D_{50} \leq 2.5 \text{ mm}$ )

**Table 7** Coefficients  $a$ ,  $c$  and  $R^2$  for Eqs. 4 and 5

Extreme sizes	$D_{50}$ (mm)	$a$	$c$	$R^2$
Group 1 ( $A_i$ , $B_i$ and $C_i$ )	1.0	7.20	61.08	0.99
$1.6 \text{ mm} \leq D_{\max} \leq 4.0 \text{ mm}$	0.63	-13.59	73.58	0.86
$D_{\min} = 0.0016 \text{ mm}$	0.25	1.58	41.83	0.98
Group 2 ( $D_i$ , $E_i$ and $F_i$ )	1.0	0.39	4.20	0.68
$D_{\max} = 4.0 \text{ mm}$	1.6	0.27	4.22	0.74
$0.0016 \text{ mm} \leq D_{\min} \leq 0.63 \text{ mm}$	2.5	0.58	4.26	0.65

minimum grain sizes ( $D_{\max}$ ,  $D_{\min}$ ) of the sandy samples under consideration:

$$q_{\max} = a * \log(D_{\max}) + c \tag{4}$$

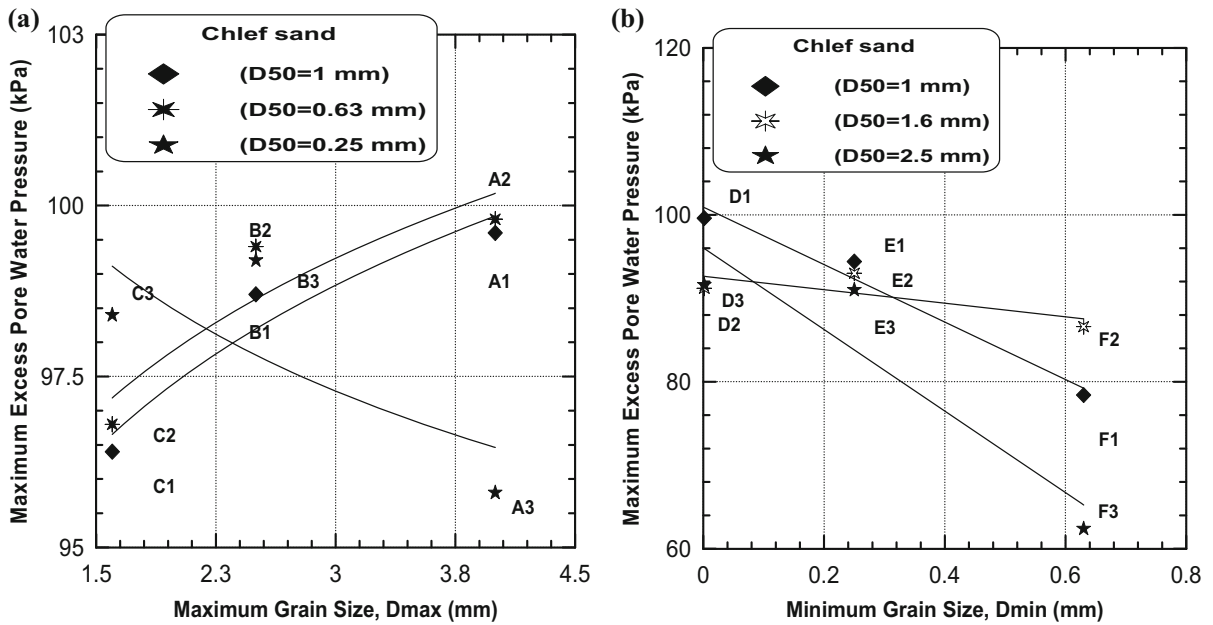
$$\log(q_{\max}) = a * \log(D_{\min}) + c \tag{5}$$

Table 7 illustrates the coefficients  $a$ ,  $c$  and the corresponding coefficient of determination ( $R^2$ ) for the selected material under consideration.

### 7 Effects of $D_{\max}$ and $D_{\min}$ on the Maximum Excess Pore Water Pressure

The effects of the extreme grain sizes ( $0.0016 \text{ mm} \leq D_{\min} \leq 0.63 \text{ mm}$ ) and ( $1.6 \text{ mm} \leq D_{\max} \leq 4.0 \text{ mm}$ ) and on the generated maximum excess pore water

pressure of saturated Chlef sand samples reconstituted at initial relative density ( $D_r = 25\%$ ) considering two different ranges of the mean grain sizes ( $0.25 \text{ mm} \leq D_{50} \leq 1.0 \text{ mm}$ ) and ( $1.0 \text{ mm} \leq D_{50} \leq 2.5 \text{ mm}$ ) are presented in Fig. 17. As it can be seen from this Fig. 17a, the trend of group 1 samples indicate that the maximum excess pore water pressure increases logarithmically with the increase of the maximum grain size ( $D_{\max}$ ) for the mean grain sizes  $D_{50} = 0.63 \text{ mm}$  and  $D_{50} = 1.0 \text{ mm}$  while the inverse tendency is observed for the samples reconstituted with the mean grain size  $D_{50} = 0.25 \text{ mm}$ . This can be attributed to the effect of the grain size distribution with higher mean grain sizes ( $D_{50} = 1 \text{ mm}$  and  $D_{50} = 0.63 \text{ mm}$ ) to increase the interlocking and consequently the decrease of the excess pore water pressure with the decrease of the maximum grain size



**Fig. 17** Maximum excess pore water pressure versus extreme grain sizes ( $D_r = 25\%$ ,  $P'_c = 100$  kPa). **a** Group 1 ( $1.6 \text{ mm} \leq D_{\max} \leq 4.0 \text{ mm}$ ,  $0.25 \text{ mm} \leq D_{50} \leq 1.0 \text{ mm}$ ). **b** Group 2 ( $0.0016 \text{ mm} \leq D_{\min} \leq 0.63 \text{ mm}$ ,  $1.0 \text{ mm} \leq D_{50} \leq 2.5 \text{ mm}$ )

**Table 8** Coefficients a, c and  $R^2$  for Eqs. 6 and 7

Extreme sizes	$D_{50}$ (mm)	a	c	$R^2$
Group 1 ( $A_i$ , $B_i$ and $C_i$ )	1.0	0.03	4.55	0.93
$1.6 \text{ mm} \leq D_{\max} \leq 4.0 \text{ mm}$	0.63	0.03	4.56	0.83
$D_{\min} = 0.0016 \text{ mm}$	0.25	-0.02	4.61	0.55
Group 2 ( $D_i$ , $E_i$ and $F_i$ )	1.0	-37.93	102.74	0.99
$D_{\max} = 4.0 \text{ mm}$	1.6	-8.11	92.65	0.61
$0.0016 \text{ mm} \leq D_{\min} \leq 0.63 \text{ mm}$	2.5	-48.86	96.02	0.86

( $D_{\max}$ ) for  $A_1, B_1, C_1$  and  $A_2, B_2, C_2$ . In Fig. 17b, the maximum excess pore water pressure ( $\Delta u_{\max}$ ) decreases linearly with the increase of minimum grain size ( $D_{\min}$ ) for all mean grain size under study (group 2). Moreover, the maximum excess pore water pressure ( $\Delta u_{\max}$ ) versus the minimum grain size ( $D_{\min}$ ) of the tested samples exhibit higher slopes (respectively  $a = 37.93$  and  $a = 48.86$ ) for the  $D_{50} = 1.0$  mm and  $D_{50} = 2.5$  mm in comparison to the intermediate mean grain size ( $D_{50} = 1.6$  mm). The maximum excess pore water pressure ( $\Delta u_{\max}$ ) could be related to extreme grain sizes ( $D_{\max}$ , and  $D_{\min}$ ) through the following relations:

$$\text{Log}(\Delta u_{\max}) = a * \text{log}(D_{\max}) + c \tag{6}$$

$$\Delta u_{\max} = a * (D_{\min}) + c \tag{7}$$

Table 8 illustrates the coefficients a, c and the corresponding coefficient of determination ( $R^2$ ) for the selected material under consideration.

### 8 Relationship Between Undrained Shear Strength and Excess Pore Water Pressure

Figure 18 shows the variation of the maximum shear strength ( $q_{\max}$ ) as a function of the maximum excess pore water pressure ( $\Delta u_{\max}$ ) considering two ranges of the mean grain sizes ( $0.25 \text{ mm} \leq D_{50} \leq 1.0 \text{ mm}$ ) and ( $1.0 \text{ mm} \leq D_{50} \leq 2.5 \text{ mm}$ ) for the initial relative density under study ( $D_r = 25\%$ ). It can be seen from Fig. 18a that the maximum shear strength ( $q_{\max}$ ) increases linearly with the increase of maximum

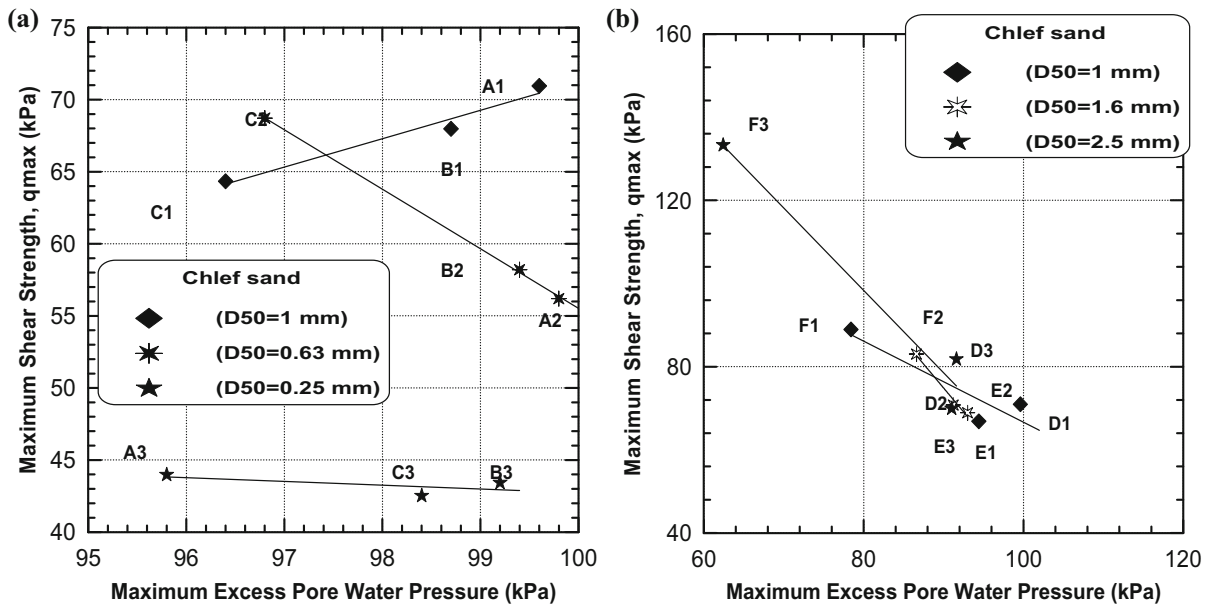


**Fig. 18** Maximum shear strength versus maximum excess pore water pressure ( $D_r = 25\%$ ,  $P'_c = 100$  kPa). **a** Group 1 ( $1.6 \text{ mm} \leq D_{\text{max}} \leq 4.0 \text{ mm}$ ,  $0.25 \text{ mm} \leq D_{50} \leq 1.0 \text{ mm}$ ). **b** Group 2 ( $0.0016 \text{ mm} \leq D_{\text{min}} \leq 0.63 \text{ mm}$ ,  $1.0 \text{ mm} \leq D_{50} \leq 2.5 \text{ mm}$ )

excess pore water pressure ( $\Delta u_{\text{max}}$ ) for  $D_{50} = 1 \text{ mm}$ , and it decreases with the increase of maximum excess pore water pressure ( $\Delta u_{\text{max}}$ ) for  $D_{50} = 0.63 \text{ mm}$ , but for  $D_{50} = 0.25 \text{ mm}$ , it remains almost the same (there is insignificant change), for group1. From Fig. 18b, we notice that the maximum shear strength ( $q_{\text{max}}$ ) increases in a linear manner with the decrease of maximum excess pore water pressure ( $\Delta u_{\text{max}}$ ) and with the increase of mean grain size  $D_{50}$  from 1 mm to 2.5 mm and for the range of the minimum grain size ( $0.0016 \text{ mm} \leq D_{\text{min}} \leq 0.63 \text{ mm}$ ) (group 2). It is observed that the ( $q_{\text{max}}$ ) correlates very well with ( $\Delta u_{\text{max}}$ ) ( $0.40 \leq R^2 \leq 0.99$  for group 01 and  $0.77 \leq R^2 \leq 0.98$  for group 02) for the sandy samples under consideration. The intermediate and higher

mean grain size ( $D_{50} = 1.6 \text{ mm}$  and  $D_{50} = 2.5 \text{ mm}$ ) generate higher undrained shear strength slope lines ( $a = 2.29$  for  $D_{50} = 1.6 \text{ mm}$  and  $a = 1.97$  for  $D_{50} = 2.5 \text{ mm}$ ) comparing to the lower mean grain size ( $D_{50} = 1.0 \text{ mm}$ ). The following equation relates the maximum shear strength ( $q_{\text{max}}$ ) with the maximum excess pore water pressure ( $\Delta u_{\text{max}}$ ) for the sandy samples prepared with different mean grain sizes and extreme grain sizes:

$$q_{\text{max}} = a * \Delta u_{\text{max}} + c \tag{8}$$

Table 9 illustrates the coefficients a, c and the corresponding coefficient of determination ( $R^2$ ) for the materials under study.

**Table 9** Coefficients a, c and  $R^2$  for Eq. 8

Extreme sizes	$D_{50}$ (mm)	a	c	$R^2$
Group 1 ( $A_i$ , $B_i$ and $C_i$ )	1.0	-1.97	-125.81	0.96
$1.6 \text{ mm} \leq D_{\text{max}} \leq 4.0 \text{ mm}$	0.63	-4.12	468.49	0.99
$D_{\text{min}} = 0.0016 \text{ mm}$	0.25	-0.26	68.77	0.40
Group 2 ( $D_i$ , $E_i$ and $F_i$ )	1.0	-0.85	154.11	0.77
$D_{\text{max}} = 4.0 \text{ mm}$	1.6	-2.29	281.47	0.98
$0.0016 \text{ mm} \leq D_{\text{min}} \leq 0.63 \text{ mm}$	2.5	-1.97	256.61	0.96

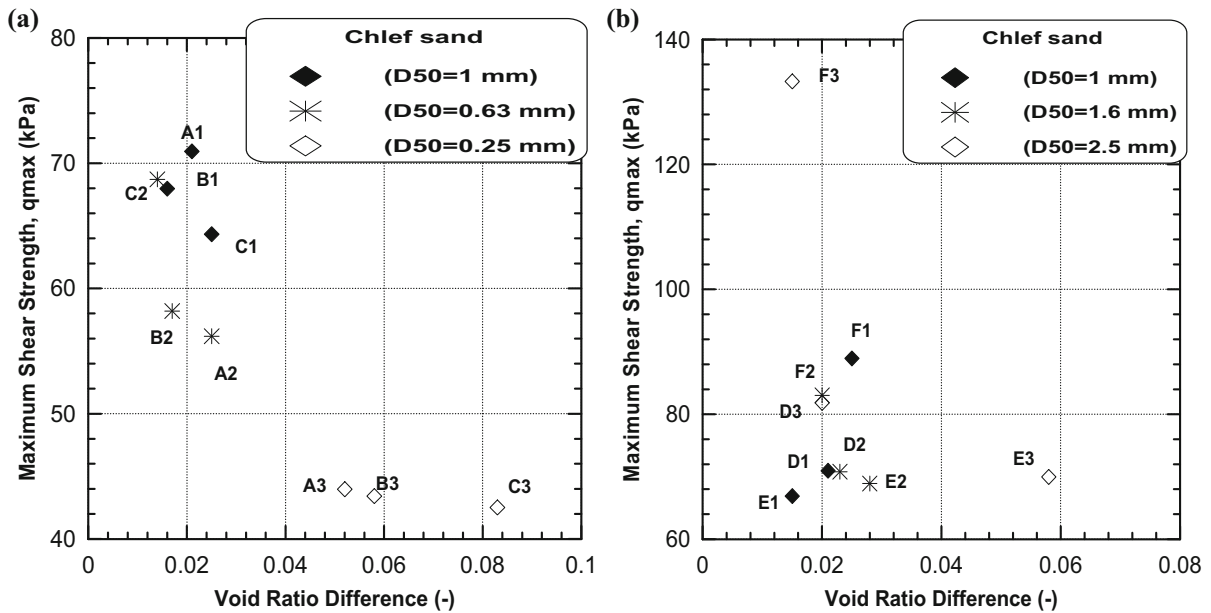


**Fig. 19** Maximum shear strength versus void ratio difference ( $D_r = 25\%$ ,  $P'_c = 100$  kPa). **a** Group 1 ( $1.6 \text{ mm} \leq D_{max} \leq 4.0 \text{ mm}$ ,  $0.25 \text{ mm} \leq D_{50} \leq 1.0 \text{ mm}$ ). **b** Group 2 ( $0.0016 \text{ mm} \leq D_{min} \leq 0.63 \text{ mm}$ ,  $1.0 \text{ mm} \leq D_{50} \leq 2.5 \text{ mm}$ )

## 9 Effects of Void Ratio Difference on the Maximum Undrained Shear Strength

For the purpose of analyzing the effects of the void ratio difference ( $\Delta e_c$ ) on the maximum shear strength ( $q_{max}$ ) of sand samples reconstituted with different mean grain sizes and different extreme grain sizes at the relative density ( $D_r = 25\%$ ) and subjected to a confining pressure of 100 kPa. Figure 19 reproduces the obtained test results indicating that samples reconstituted with a maximum grain size range of ( $1.6 \text{ mm} \leq D_{max} \leq 4 \text{ mm}$ ) exhibit an increase of the maximum shear strength with the decrease of void ratio difference as  $D_{max}$  increases from 1.6 mm to 4.0 mm for soils with mean grain sizes of ( $D_{50} = 1 \text{ mm}$ ,  $0.25 \text{ mm}$ ). For the intermediate mean grain size ( $D_{50} = 0.63 \text{ mm}$ ), the maximum shear strength ( $q_{max}$ ) decreases with the increase of void ratio difference and  $D_{max}$  from 1.6 mm to 4 mm. For group 2, the maximum shear strength decreases with the decrease of void ratio difference for  $D_{50} = 1 \text{ mm}$  and that of  $D_{min}$  from 0.63 mm to 0.0016 mm. Moreover, the maximum shear strength decreases with the decrease of the void ratio difference as the

mean grain size ranges between  $D_{50} = 1.6 \text{ mm}$  and 2.5 mm and  $D_{min}$  from 0.63 mm to 0.0016 mm.

## 10 Effects of $D_{50}$ on the Maximum Undrained Shear Strength

The test results obtained from the current study (Figs. 8, 9, 10, 11, 12, 13) illustrate the effects of the mean grain size ( $D_{50}$ ) on the maximum undrained shear strength (Fig. 20) considering two ranges of the extreme grain sizes ( $1.6 \text{ mm} \leq D_{max} \leq 4.0 \text{ mm}$  for group 1 and  $0.0016 \text{ mm} \leq D_{min} \leq 0.63 \text{ mm}$  for group 2). It is clear from Fig. 20a that the maximum undrained shear strength increases logarithmically in a similar manner with the increase of the mean grain size for the range of the maximum grain size range under consideration ( $1.6 \text{ mm} \leq D_{max} \leq 4.0 \text{ mm}$ ). It is observed from Fig. 20a that the mean grain size affects in a similar way the  $q_{max}-D_{50}$  response of the tested soil samples for the range of the maximum grain size under consideration and the maximum grain size ( $D_{max}$ ) has no discernible effect on the  $q_{max}-D_{50}$  response of ( $A_i$ ,  $B_i$  and  $C_i$ ) samples. This means that

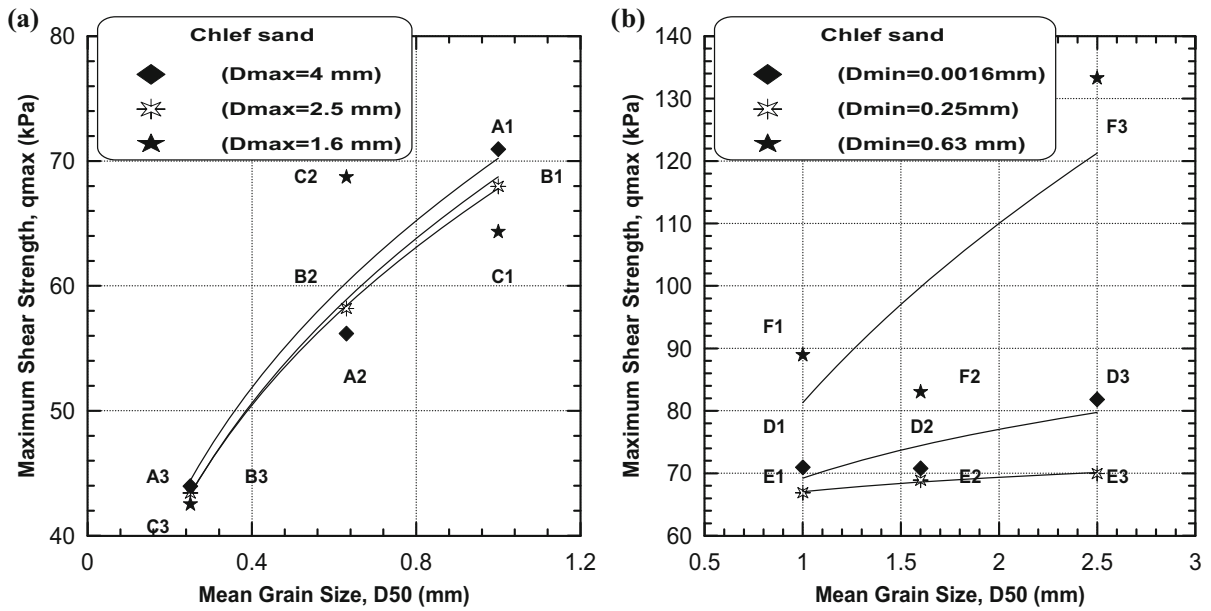


**Fig. 20** Maximum shear strength versus mean grain size ( $D_r = 25\%$ ,  $P'_c = 100$  kPa). **a** Group 1 ( $1.6 \text{ mm} \leq D_{\text{max}} \leq 4.0 \text{ mm}$ ,  $D_{\text{min}} = 0.0016 \text{ mm}$ ). **b** Group 2 ( $D_{\text{max}} = 4.0 \text{ mm}$ ,  $0.0016 \text{ mm} \leq D_{\text{min}} \leq 0.63 \text{ mm}$ )

the maximum undrained shear strength response of the different sandy samples is much more influenced by the mean grain size ( $D_{50}$ ) than by the maximum grain size ( $D_{\text{max}}$ ). For the different samples of group 1, the one with the smaller effective grain size ( $D_{10}$ ) and mean grain size ( $D_{50}$ ) is the more susceptible to liquefaction. This is parallel to the findings of Yilmaz and Mollamahmutoglu (2009). For the samples of group 2 ( $D_{\text{max}} = 4.0 \text{ mm}$ ,  $0.0016 \text{ mm} \leq D_{\text{min}} \leq 0.63 \text{ mm}$ ), the mean grain size affects considerably the undrained shear strength, particularly the  $F_i$  samples reconstituted with higher  $D_{\text{min}} = 0.63 \text{ mm}$ . However, the other two set samples ( $D_i$  and  $E_i$ ) show a moderate undrained shear strength increase with the increase of the mean grain size. This small increase may result from the role of the presence of the fines fraction ( $0.0016 \text{ mm} \leq D_{\text{min}} \leq 0.25 \text{ mm}$ ) within the grain size distribution in increasing the contractiveness of the different sand samples for the considered initial relative density ( $D_r = 25\%$ ), which leads to an increase of the excess pore water pressure and consequently to a decrease of the undrained shear strength. The results of this study show that the undrained shear strength of the different sand samples could be correlated to the mean grain size ( $D_{50}$ ) for the range of the extreme grain sizes tested and relative

density under consideration. This is parallel to the findings of (Ishihara et al. 1975; Castro and Poulos 1977; Belkhatir et al. 2014; Cherif Taiba et al. 2016). The maximum undrained shear strength could be related to the mean grain size through the following relation:

$$\text{Log}(q_{\text{max}}) = a * \text{log}(D_{50}) + c \tag{9}$$

Table 10 illustrates the coefficients  $a$ ,  $c$  and the corresponding coefficient of determination ( $R^2$ ) for the materials under study.

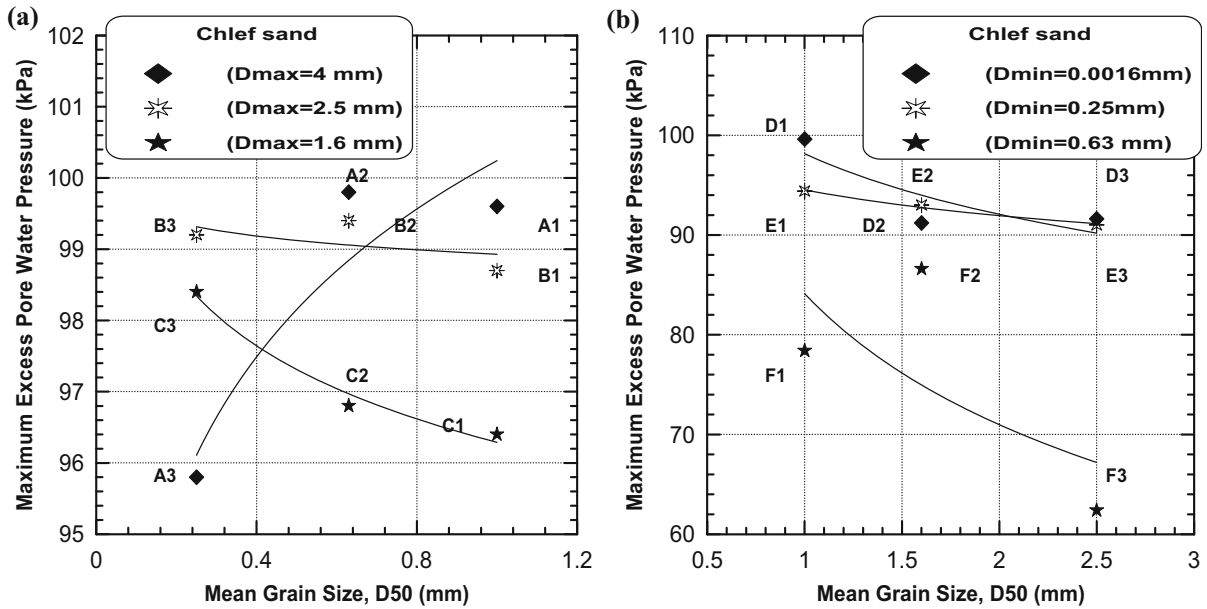
### 11 Effect of $D_{50}$ on the Maximum Excess Pore Water Pressure

Figure 21 also reproduces the data from the current laboratory investigation indicating that the samples  $B_i$  and  $C_i$  exhibit a decrease of the maximum excess pore water pressure with the increase of the mean grain size  $D_{50}$  while  $A_i$  samples exhibit an increase of the maximum excess pore water pressure with the increase of the mean grain size  $D_{50}$ . The effects of  $D_{\text{max}}$  combined with  $D_{50}$  (group 1) on the undrained shear strength are clearly observed rather than the  $D_{\text{min}}$  combined with  $D_{50}$  (group 2). As can be seen from



**Table 10** Coefficients a, c and R<sup>2</sup> for Eq. (9)

Extreme sizes	D <sub>max</sub> or D <sub>min</sub> (mm)	a	c	R <sup>2</sup>
Group 1 (A <sub>i</sub> , B <sub>i</sub> and C <sub>i</sub> )	4.0	0.33	4.23	0.96
1.6 mm ≤ D <sub>max</sub> ≤ 4.0 mm	2.5	0.33	4.21	0.99
D <sub>min</sub> = 0.0016 mm	1.6	0.33	4.25	0.80
Group 2 (D <sub>i</sub> , E <sub>i</sub> and F <sub>i</sub> )	0.0016	0.15	4.23	0.72
D <sub>max</sub> = 4.0 mm	0.25	0.04	4.20	0.97
0.0016 mm ≤ D <sub>min</sub> ≤ 0.63 mm	0.63	0.43	4.39	0.61



**Fig. 21** Maximum excess pore water pressure versus mean grain size ( $D_r = 25\%$ ,  $P'_c = 100$  kPa). **a** Group 1 ( $1.6 \text{ mm} \leq D_{\text{max}} \leq 4.0 \text{ mm}$ ,  $D_{\text{min}} = 0.0016 \text{ mm}$ ). **b** Group 2 ( $D_{\text{max}} = 4.0 \text{ mm}$ ,  $0.0016 \text{ mm} \leq D_{\text{min}} \leq 0.63 \text{ mm}$ )

**Table 11** Coefficients a, c and R<sup>2</sup> for Eq. (10)

Extreme sizes	D <sub>max</sub> or D <sub>min</sub> (mm)	a	c	R <sup>2</sup>
Group 1 (A <sub>i</sub> , B <sub>i</sub> and C <sub>i</sub> )	4.0	0.03	4.60	0.86
1.6 mm ≤ D <sub>max</sub> ≤ 4.0 mm	2.5	−0.02	4.59	0.30
D <sub>min</sub> = 0.0016 mm	1.6	−0.015	4.56	0.98
Group 2 (D <sub>i</sub> , E <sub>i</sub> and F <sub>i</sub> )	0.0016	−0.09	4.58	0.72
D <sub>max</sub> = 4.0 mm	0.25	−0.03	4.54	0.98
0.0016 mm ≤ D <sub>min</sub> ≤ 0.63 mm	0.63	−0.24	4.43	0.44

Fig. 21a the generated excess pore water pressure decreases with the increase of the mean grain size for B<sub>i</sub> and C<sub>i</sub> set of samples. The inverse tendency is observed for A<sub>i</sub> samples. Figure 21b shows a decrease of the maximum excess pore water pressure with the

increase of the mean grain size. However, the minimum grain size (D<sub>min</sub>) has no apparent effect on the maximum excess pore water pressure of D<sub>i</sub> and E<sub>i</sub> samples in comparison to F<sub>i</sub> samples. The larger D<sub>min</sub> = 0.63 mm exhibits significant decrease of the

maximum excess pore water pressure for Fi samples rather than the lower  $D_{\min} = 0.0016$  mm and  $D_{\min} = 0.25$  mm respectively for Di and Ei samples. This is due to the presence of the fine-grained soil fraction ( $0.0016 \text{ mm} \leq D_{\min} \leq 0.63 \text{ mm}$ ) within the grain size distribution of Di and Ei samples. The maximum excess pore water pressure could be related to the mean grain size through the following relation:

$$\text{Log}(\Delta u_{\max}) = a * \text{log}(D_{50}) + c \quad (10)$$

Table 11 illustrates the coefficients  $a$ ,  $c$  and the corresponding coefficient of determination ( $R^2$ ) for the materials under study.

## 12 Conclusion

The present laboratory investigation is based upon a series of undrained monotonic compression triaxial tests to study the effects of the extreme grain sizes ( $D_{\max}$  and  $D_{\min}$ ) and mean grain size ( $D_{50}$ ) on the undrained shear strength (known as static liquefaction) response of saturated Chlef sand samples prepared with wet deposition technique at an initial relative density ( $D_r = 25\%$ ) and subjected to a constant confining pressure of 100 kPa. In light of the experimental evidence, the following conclusions can be drawn:

1. The obtained test results indicate clearly that the extreme grain sizes ( $D_{\max}$  and  $D_{\min}$ ) combined with the mean grain size ( $D_{50}$ ) control in a significant manner the undrained shear (static liquefaction resistance) response.
2. The extreme grain sizes ( $D_{\max}$  and  $D_{\min}$ ) can be correlated to the generated extreme void ratios ( $e_{\max}$  and  $e_{\min}$ ) for the two ranges of the mean grain size ( $0.25 \text{ mm} \leq D_{50} \leq 1.0 \text{ mm}$ ,  $1.0 \text{ mm} \leq D_{50} \leq 2.5 \text{ mm}$ ) of the sandy samples under study.
3. The post-consolidation void ratio decreases in logarithmic manner with the increase of maximum grain size ( $D_{\max}$ ), however, it increases logarithmically with the increase of minimum grain size ( $D_{\min}$ ) for the selected mean grain sizes.
4. Flow and limited flow behavior cases of wet deposited samples are observed for all the extreme grain sizes and mean grain sizes ( $0.25 \text{ mm} \leq D_{50} \leq 1.0 \text{ mm}$ ,  $1.0 \text{ mm} \leq D_{50} \leq 2.5 \text{ mm}$ ) ranges

under consideration. The present outcome is in good agreement with the results of Benahmed et al. (2004), Della et al. (2014a, b).

5. The maximum shear strength and excess pore water pressure can be correlated to the extreme grain sizes ( $D_{\max}$  and  $D_{\min}$ ) by a good logarithmic and linear relationship for all mean grain sizes used in this study for the tested sandy samples.
6. The higher and lower mean grain sizes ( $D_{50} = 1.0 \text{ mm}$ ,  $D_{50} = 0.25 \text{ mm}$ ) exhibit a decrease of the maximum undrained shear strength with the decrease of the maximum grain size ( $D_{\max}$ ), while the intermediate mean grain size ( $D_{50} = 0.63 \text{ mm}$ ) shows the inverse soil trend for group 01
7. The trend of group 1 samples indicate that the maximum excess pore water pressure increases logarithmically with the increase of the maximum grain size ( $D_{\max}$ ) for the mean grain sizes  $D_{50} = 0.63 \text{ mm}$  and  $D_{50} = 1.0 \text{ mm}$  while the inverse tendency is observed for the samples reconstituted with the mean grain size  $D_{50} = 0.25 \text{ mm}$ .

**Acknowledgements** This laboratory research work was supported by Alexander von Humboldt Foundation (AvH) through Georg Forster Research Program grant funded by the German government for the third author. It was carried out in the Laboratory of Foundation Engineering, Soil and Rock Mechanics at Ruhr University of Bochum (Germany). The authors are grateful to the technician Werner Müller for his valuable contribution in the execution of this experimental program. The authors are also grateful to the anonymous reviewers for their critical review and suggestions.

## References

- Amini F, Qi GZ (2000) Liquefaction testing of stratified silty sands. *J Geotech Geoenviron Eng Proc ASCE* 126(3):208–217
- ASTM D 4253-00 (2002) "Standard test method for maximum index density and unit weight of soils using a vibratory table". Annual Book of ASTM Standards. American Society for Testing and Materials, West Conshohocken, pp 1–14
- ASTM D 4254-00 (2002) "Standard test method for minimum index density and unit weight of soils and calculation of relative density". Annual Book of ASTM Standards. American Society for Testing and Materials, West Conshohocken, pp 1–9
- Bayat M, Bayat E (2012) Effect of grading characteristics on the undrained shear strength of sand: review with new evidences. *Arab J Geosci*. doi:10.1007/s12517-012-0670-y

- Belkhatir M, Arab A, Della N, Missoum H, Schanz T (2010) Liquefaction resistance of Chlef river silty sand: effect of low plastic fines and other parameters. *Acta Polytech Hung* 7(2):119–137
- Belkhatir M, Arab A, Missoum H, Della N, Schanz T (2011) Laboratory study on the liquefaction resistance of sand–silt mixtures: effect of grading characteristics. *Granul Matter* 13:599–609
- Belkhatir M, Arab A, Della N, Schanz T (2012) Experimental study of undrained shear strength of silty sand: effect of fines and gradation. *Geotech Geol Eng* 30(5):1103–1118
- Belkhatir M, Schanz T, Arab A, Della N, Kadri A (2014) Insight into the effects of gradation on the pore pressure generation of sand–silt mixtures. *Geotech Test J* 37(5):922–931
- Benahmed N, Canou J, Dupla JC (2004) Structure initiale et propriétés de liquéfaction statique d'un sable. *C R Mécanique* 332:887–894
- Benghalia Y, Bouafia A, Canou J, Dupla JC (2014) Liquefaction susceptibility study of sandy soils: effect of low plastic fines. *Arab J Geosci*. doi:[10.1007/s12517-013-1255-0](https://doi.org/10.1007/s12517-013-1255-0)
- Carraro JAH, Prezzi M (2008) A New Slurry-Based Method of Preparation of Specimens of Sand Containing Fines. *Geotech Test J ASTM* 31(1):1–11
- Castro G, Poulos SJ (1977) Factors affecting liquefaction and cyclic mobility. *J Geotech Eng* 103(GT6):501–516
- Chang NY, Yeh ST, Kaufman LP (1982) Liquefaction potential of clean and silty sands. In: *Proceedings of 3rd international earthquake microzonation conference*, vol 2, pp 1017–1032
- Chang CS, Wang JY, Ge L (2016) Maximum and minimum void ratios for sand–silt mixtures. *Eng Geol* 211:7–18
- Cherif Taiba A, Belkhatir M, Kadri A, Mahmoudi Y, Shanz T (2016) Insight into the effect of granulometric characteristics on the static liquefaction susceptibility of silty sand soils. *Geotech Geol Eng* 34(1):367–382
- Choobbasti JA, Ghalandarzadeh A, Esmaeili M (2013) Experimental study of the grading characteristic effect on the liquefaction resistance of various graded sands and gravelly sands. *Arabian J Geosci*. doi:[10.1007/s12517-013-0886-5](https://doi.org/10.1007/s12517-013-0886-5)
- Cubrinovski M, Ishihara K (2002) Maximum and minimum void ratio characteristics of sands. *Soils Found* 42(6):65–78
- Della N, Arab A, Belkhatir M (2011) Static liquefaction of sandy soil: an experimental investigation into the effects of saturation and initial state. *Acta Mech* 218(1–2):175–186
- Della N, Belkhatir M, Arab A, Canou J, Dupla JC (2014a) Effect of fabric method on instability behavior of granular material. *Acta Mech* 225:2043–2057
- Della N, Belkhatir M, Arab A, Canou J, Dupla JC (2014b) Undrained monotonic response and instability of medium dense sandy soil. *Mar Georesour Geotechnol* 33(6):141217134114005
- Djafar Henni A, Arab A, Belkhatir M, Hamoudi SA, Khelafi H (2011) Undrained behavior of silty sand: effect of the overconsolidation ratio. *Arab J Geosci*. doi:[10.1007/s12517-011-0365-9](https://doi.org/10.1007/s12517-011-0365-9)
- Finn WDL, Bransby PL, Pickering DJ (1970) Effect of strain history on liquefaction of sand. *J Soil Mech Found ASCE* 96(SM6):1917–1934
- Frost JD, Park JY (2003) A critical assessment of the moist tamping technique. *J Geotech Test* 26(1):1–14
- Høeg K, Dyvik R, Sandbækken G (2000) Strength of undisturbed versus reconstituted silt and silty sand specimens. *J Geotech Geoenviron Eng* 126(7):606–617. doi:[10.1061/\(ASCE\)1090-0241\(2000\)126:7\(606\)](https://doi.org/10.1061/(ASCE)1090-0241(2000)126:7(606))
- Igwe O, Fukuoka H, Sassa K (2012) The effect of relative density and confining stress on shear properties of sands with varying grading. *Geotech Geol Eng* 30:1207–1229
- Ishihara K (1993) Liquefaction and flow failure during earthquakes. *Geotechnique* 43(3):351–415
- Ishihara K, Tatsuoka F, Yasuda S (1975) Undrained deformation and liquefaction of sand under cyclic stresses. *Soil Found* 15(1):29–44
- Jafarian Y, Ghorbani A, Salamatpoor S (2013) Monotonic triaxial experiments to evaluate steady-state and liquefaction susceptibility of Babolsar sand. *J Zhejiang Univ-Sci A (Appl Phys Eng)* 14(10):739–750
- Janalizadeh CA, Ghalandarzadeh A, Esmaeili M (2013) Experimental study of the grading characteristic effect on liquefaction resistance of various graded sands and gravelly sands. *Arab Geosci*. doi:[10.1007/s12517-013-0886-5](https://doi.org/10.1007/s12517-013-0886-5)
- Kanagalingam T, Thevanayagam S (2005) Discussion to “Contribution of fines to the compressive strength of mixed soils”. *Geotechnique* 55(8):627–628
- Kokusho T, Hara T, Hiraoka R (2004) Undrained shear strength of granular soils with different particle gradations. *J Geotech Geoenviron Eng* 130:621–629
- Lade PV, Duncan JM (1973) Cubical triaxial tests on cohesionless soil. *J Soil Mech Found Eng Div* 99(10):793–812
- Lade PV, Yamamuro JA (1997) Effects of non-plastic fines on static liquefaction of sands. *Can Geotech J* 34:918–928
- Lee KL, Fitton JA (1968) Factors affecting the cyclic strength of soil. *Vibration effects on earthquakes on soils and foundations*. ASTM STP 450:71–95
- Liu YJ, Li G, Zhen YY, Dano C, Hicher PY, Xiao HX, Wang JH (2014) “Influence of grading on the undrained behavior of granular materials” symposium about “Recent Advances in the Mechanics of Granular and Porous Media” at the European Solid Mechanics Conference in Graz, Austria
- Mahmoudi Y, Cherif Taiba A, Belkhatir M, Schanz T (2016) Experimental investigation on undrained shear behavior of over consolidated sand–silt mixtures: effect of sample reconstitution. *Geotech Test J* 39(3):515–523. doi:[10.1520/GTJ20140183](https://doi.org/10.1520/GTJ20140183)
- Missoum H, Belkhatir M, Bendani K (2011) Undrained shear strength response under monotonic loading of Chlef (Algeria) sandy soil. *Arab J Geosci*. doi:[10.1007/s12517-011-0387-3](https://doi.org/10.1007/s12517-011-0387-3)
- Miura S, Toki S, Tatsuoka F (1994) Cyclic undrained triaxial behavior of sand by a cooperative test program in Japan. In: Ebelhar RJ, Drenvich VP, Kutter BL (eds) *Dynamic geotechnical testing II*, ASTM STP, vol 1213, pp 246–260
- Miura K, Maeda K, Furukawa M, Toki S (1997) Physical characteristics of sands with different primary properties. *Soils Found* 37(3):53–64
- Monkul MM, Yamamuro JA (2011) Influence of silt size and content on liquefaction behavior of sands. *Can Geotech J* 48:931–942
- Monkul MM, Etmnan E, Senol A (2016) Influence of coefficient of uniformity and base sand gradation on static

- liquefaction of loose sand with silt. *Soil Dyn Earthq Eng* 89:185–197
- Naeini SA (2001) The influence of silt presence and sample preparation on liquefaction potential of silty sands. Ph.D. Dissertation, Iran University of Science and Technology, Tehran, Iran
- Naeini SA, Baziar MH (2004) Effect of fines content on steady-state strength of mixed and layered samples of a sand. *Soil Dyn Earthq Eng* 24:181–187
- Sadrekarami A (2013) Influence of fines content on liquefied strength of silty sands. *Soil Dyn Earthq Eng* 55:108–119
- Sadrekarami A, Olson SM (2012) Effect of Sample-Preparation Method on Critical-State Behavior of Sands. *Geotech Test J* 35(4):1–15
- Seed HB, Idriss IM (1971) A simplified procedure for evaluating soil liquefaction potential. *J Soil Mech Found Eng ASCE* 97(9):1249–1274
- Seed HB, Peacock WH (1971) Test procedures for measuring soil liquefaction characteristics. *J Soils Mech Found Div ASCE* 97(8):1099–1119
- Sharafi H, Baziar MH (2010) A laboratory study on the liquefaction resistance of Firouzkoo silty sands using hollow torsional system. *EJGE* 15:973–982
- Sze HY, Yang J (2014) Failure modes of sand in undrained cyclic loading: impact of sample preparation. *J Geotech Geoenviron Eng* 140:152–169
- Thevanayagam S (1998) Effect of fines and confining stress on undrained shear strength of silty sands. *J Geotech Geoenviron Eng Div ASCE* 124(6):479–491
- Thevanayagam S, Ravishankar K, Mohan S (1997) Effects of fines on monotonic undrained shear strength of sandy soils. *ASTM Geotech Test J* 20(1):394–406
- Vaid YP, Fisher JM, Kuerbis RH (1991) Particle gradation and liquefaction. *J Geotech Eng* 116(4):698–703
- Vaid YP, Sivathayalan S, Stedman D (1999) Influence of specimen reconstituting method on the undrained response of sand. *Geotech Test J* 22(3):187–195
- Yamamoto JA, Lade PV (1998) Steady-state concepts and static liquefaction of silty sands. *J Geotech Geoenviron Eng ASCE* 124(9):868–877
- Yamamoto JA, Wood FM (2004) Effect of depositional method on the undrained behavior and microstructure of sand with silt. *Soil Dyn Earthq Eng* 24:751–760
- Yanrong L (2013) Effects of particle shape and size distribution on the shear strength behavior of composite soils. Springer, New York
- Yilmaz Y, Mollamahmutoglu M (2009) Characterisation of liquefaction susceptibility of sands by means of extreme void ratios and/or void ratio range. *J Geotech Geoenviron Eng* 135(12):1986–1990
- Yilmaz Y, Mollamahmutoglu M, Ozaydin V, Kayabali (2008) Experimental investigation of effect of grading characteristics on the liquefaction resistance of various graded sands. *Eng Geol J* 100:91–100
- Zlatovic S, Ishihara K (1995) On the influence of non-plastic fines on residual strength. In: Proceedings of the first international conference on earthquake geotechnical engineering, Tokyo, pp 14–16